Unclassified

SECURITY CLASSIFICATION OF THIS PAGE

REPORT DOCUMENTATION PAGE

1a. REPORT SECURITY CLASSIFICATION: None	1b. RESTRICTIVE MARKINGS: None
2a. SECURITY CLASSIFICATION AUTHORITY	3. DISTRIBUTION/AVAILABILITY OF REPORT: Distribution unlimited; approved for public release
2b. DECLASSIFICATION/DOWNGRADING SCHEDULE	
4. PERFORMING ORGANIZATION REPORT NUMBER(S): SBIL-C94	5. MONITORING ORGANIZATION REPORT NUMBER(S)
6a. NAME OF PERFORMING ORGANIZATION: State University of New York at Stony Brook; 6b. OFFICE SYMBOL (If applicable)	7a. NAME OF MONITORING ORGANIZATION: Office of Naval Research
6c. ADDRESS (City, State and ZIP Code): Department of Chemistry, University at Stony Brook, Stony Brook, New York 11794-3400	7b. ADDRESS (City, State and ZIP Code): Mechanics and Energy Conversion Division, ONR 333, 800 N. Quincy Street, Arlington, Virginia 22217
8a. NAME OF FUNDING/SPONSORING ORGANIZATION; 8b. OFFICE SYMBOL (If applicable)	9. PROCUREMENT INSTRUMENT IDENTIFICATION NUMBER: N0001492-J-1202
8c. ADDRESS (City, State and ZIP Code): Mechanics and Energy Conversion Division, ONR 333, 800 N. Quincy Street, Arlington, Virginia 22217	10. SOURCE OF FUNDING NOS. — PROGRAM ELEMENT NO.; PROJECT NO.; TASK NO.; WORK UNIT NO.
11. TITLE (Include Security Classification): A Cluster Beam Study of Boron Oxide Chemistry with HF (None)	
12. PERSONAL AUTHOR(S): J. Smolanoff, A. Lapicki, S. Anderson	
13a. TYPE OF REPORT: interim; 13b. TIME COVERED: FROM _____ TO _____	14. DATE OF REPORT (Yr., Mo., Day): 941226; 15. PAGE COUNT: 37
16. SUPPLEMENTARY NOTATION	
17. COSATI CODES — FIELD; GROUP; SUB. GR.	18. SUBJECT TERMS (Continue on reverse if necessary and identify by block number): Boron Combustion, Propulsion, Boron Oxides, Clusters

DTIC ELECTED FEB 09 1995 B

19. ABSTRACT (Continue on reverse if necessary and identify by block number)

Using an improved version of the Cluster Beam technique, we have probed the chemistry of $B_xO_yH_z^+$ clusters with HF as a function of the B:O:H stoichiometry of the cluster reactant. Reactant compositions were varied from pure boron to stoichiometric oxide, with and without added hydrogen. Boron oxide clusters react with HF at about 50% efficiency and the collision energy dependence suggests that the reaction is sterically hindered, i.e. reaction occurs primarily at certain sites in the oxide network. The principle reaction is attack by the HF on a terminal BO group, followed by loss of fragments such as FBOH and FBO. Addition of a single hydrogen atom has a significant effect on the chemistry. The products of the reaction (and probably the mechanism) are similar to those for the pure oxides, but the reactivity is substantially reduced. We propose that the hydrogen atom blocks a reactive site on the cluster, thereby reducing the reactivity. Pure boron clusters react by addition of HF, followed by elimination of fragments such as BF and HBF. For small clusters the reaction is efficient, but we see activation barriers grow in for the larger clusters, suggesting that there may be activation barriers for boron surface-HF reactions as well. In contrast to the situation for the oxides, addition of hydrogen to the pure boron clusters generally *increases* the reactivity with HF.

20. DISTRIBUTION/AVAILABILITY OF ABSTRACT: UNCLASSIFIED/UNLIMITED ☒ SAME AS RPT. ☐ DTIC USERS ☐	21. ABSTRACT SECURITY CLASSIFICATION: None
22a. NAME OF RESPONSIBLE INDIVIDUAL: Dr. Richard S. Miller	22b. TELEPHONE NUMBER (Include Area Code): 703 696-4404; 22c. OFFICE SYMBOL

DD FORM 1473, 83 APR EDITION OF 1 JAN 73 IS OBSOLETE.

None

SECURITY CLASSIFICATION OF THIS PAGE

A Cluster Beam Study of Boron, Boron Oxide and B_xO_yH chemistry with Hydrogen Fluoride

Jason Smolanoff, Adam Lapicki, Marianne Sowa-Resat, and Scott L. Anderson*
Department of Chemistry, SUNY at Stony Brook, Stony Brook, NY 11794-3400

ABSTRACT

Using an improved version of the Cluster Beam technique, we have probed the chemistry of $B_xO_yH_z^+$ clusters with HF as a function of the B:O:H stoichiometry of the cluster reactant. Reactant compositions were varied from pure boron to stoichiometric oxide, with and without added hydrogen. Boron oxide clusters react with HF at about 50% efficiency and the collision energy dependence suggests that the reaction is sterically hindered, i.e. reaction occurs primarily at certain sites in the oxide network. The principle reaction is attack by the HF on a terminal BO group, followed by loss of fragments such as FBOH and FBO. Addition of a single hydrogen atom has a significant effect on the chemistry. The products of the reaction (and probably the mechanism) are similar to those for the pure oxides, but the reactivity is substantially reduced. We propose that the hydrogen atom blocks a reactive site on the cluster, thereby reducing the reactivity. Pure boron clusters react by addition of HF, followed by elimination of fragments such as BF and HBF. For small clusters the reaction is efficient, but we see activation barriers grow in for the larger clusters, suggesting that there may be activation barriers for boron surface-HF reactions as well. In contrast to the situation for the oxides, addition of hydrogen to the pure boron clusters generally *increases* the reactivity with HF. For comparison we also present survey results for chemistry of oxides and pure boron clusters with hydrogen and water.

I. Introduction

Because of its high volumetric and gravimetric energy density, boron has tremendous potential as a component in propellants and explosives. Several problems are encountered when using boron in practical applications. A passivating oxide layer forms on the boron particle surface, and this oxide melts and thickens as the particle is heated. The oxide layer impedes particle ignition and can cause agglomeration of individual boron particles; both effects tending to reduce the combustion rate and efficiency. Another problem is that the recoverable $\Delta H_{combustion}$ is reduced if undesirable products (HOBO and its polymers) form instead of the more stable B_2O_3.

A potential solution to these problems is to fluorinate one or more components of the propellant/explosive composition. During combustion, this fluorine is converted to gaseous species, such as HF, that can attack and volatilize the boron particles or their oxide coatings. This attack is likely to be relatively efficient because boron-fluorine bonds are quite strong. For the same reason, fluorine addition may improve overall energy release due to formation of more stable products. For example, since B-F bonds are substantially stronger than B-H bonds, the presence of fluorine should favor production of fluorinated boron oxides (or possibly even BF_3) rather than the undesirable HOBO products. To evaluate and optimize this approach, ONR is currently supporting an effort to model the homogenous and heterogenous chemistry of the B/O/H/C/F system. The purpose of our efforts, and of this report, is to provide insight and kinetic information regarding the largely unknown heterogeneous chemistry.

We previously reported[1] a study of the $B_nO_m^+$ + HF reaction. In the course of that work, done with isotopically purified $^{10}B_2O_3$, we observed small mass peaks one amu above the main peaks of the reactant and product species. Because the samples had been thoroughly vacuum degased at high temperatures, we attributed these peaks to ^{11}B isotope contamination. That study pointed out the need to significantly improve the mass resolution of our Cluster Beam instrument, which has been done. Using the improved apparatus, we have discovered that these small M+1 mass peaks are partly due to mono-hydrogenated boron oxide clusters, which react quite differently from the pure oxides. Given that there is plenty of hydrogen available in combustion environments (as OH, H, or H_2O) we felt that the chemistry of these species needed to be understood. Based on the results, we feel that these species should probably be included in the heterogeneous combustion models.

In this report, we present a thorough study of the chemistry of boron oxide clusters ($B_nO_m^+$) and of $B_nO_mH_p^+$ with HF. Preliminary results are also reported for reactions with D_2 and D_2O. For comparison, we present a sampling of results for the B_n^+ + HF and B_nH^+ + HF systems. We report the observed cross sections as a function of collision energy, kinetic parameters derived from the cross sections, and a discussion of possible reaction mechanisms.

II. Properties of Boron Oxide and Sample Preparation

In considering the reaction results, it is helpful to know something about the structure of boron oxide. The structure of crystalline B_2O_3 has been determined by Gurr[2] using x-ray diffraction. Three oxygen atoms surround each boron atom and each unit cell is interconnected by an oxygen 'ribbon'. Upon heating above 450 °C B_2O_3 converts to the vitreous form, which will not revert back upon cooling.

The structure of the vitreous form of B_2O_3 has been determined using ^{10}B, ^{11}B, ^{17}O NMR[3], and using x-ray diffraction[4]. These experiments suggest that the vitreous form consists of boroxyl rings (B_3O_3) interconnected by BO_3 units. Doyle[5] (NRL), has proposed structures for boron oxide cluster ions based upon his Collision Induced Dissociation (CID) studies. He proposed several resonance structures consisting of alternating boron-oxygen bonds terminated by B=O groups. The boron atom can have two or three fold coordination to oxygen atoms. The structural prototype for all of the boron oxide cluster ions is $B_3O_4^+$ $[O{=}B{-}O{-}B{-}O{-}B{=}O]^+$.

We have modified a source developed by Doyle[5] to generate $B_nO_m^+$ clusters. Isotopically pure (94%^{10}B) B_2O_3 crystalline powder was sprinkled onto a stainless steel substrate and heated in a furnace at 650°C for ~ 3-4 hours. During the heating, the furnace is purged with O_2 to keep the heating environment relatively free of water vapor. The sample is then heated in vacuum (~450°C) to further remove water. We have found boron oxide to be incredibly hygroscopic. Even in high vacuum (10^{-7} torr), our samples begin to show hydrogen contamination (presumably from absorption of trace amounts of water[6]) unless they are maintained just above the B_2O_3 melting point.

III. Experimental Approach

The ion cluster beam apparatus (see inset) and experimental methodology used for these

studies have been described previously[7,8], and only a brief description is given here. $B_nO_m^+$ clusters were produced by 12 KeV argon atom bombardment of a thin film of vitreous B_2O_3 maintained at a temperature just above its melting point. The cluster ions are collected by a radio-frequency octapole field, and then stored in an ion trap to allow thermalization by helium buffer gas. The cluster of interest is mass selected using a quadrupole mass filter. The reactant cluster ion beam is then guided into a reaction cell filled with 0.05 mTorr HF (preliminary reactions were also conducted using D_2 (0.05 mTorr), and D_2O (0.025mTorr). Products are mass analyzed using a second quadrupole filter, and detected using a Daly detector and photomultiplier.

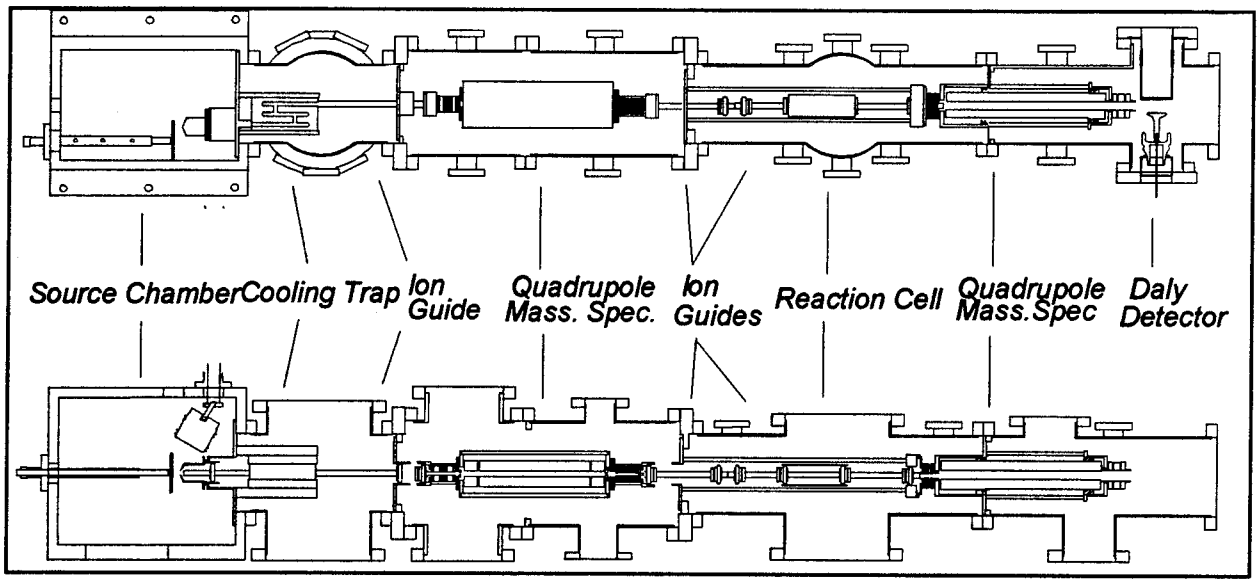

The apparatus has been upgraded by installing a quadrupole mass filter for primary reactant beam selection. Quadrupole mass filters have several desirable features, but there is a serious problem as well. When operated at moderate to high mass resolution, the translational energy distribution of the transmitted beam can be severely distorted as it passes through the strong radio-frequency and DC fields present in the quadrupole. This effectively has made this type of mass spectrometer useless for high resolution beam experiments like ours. We had the idea that by using a set of separately controlled pre- and post-filters we could beat this problem. After considerable experimentation, we found that good energy and mass resolution can be achieved simultaneously using carefully designed ion injection and collection optics. For the data presented, typical primary beam energy widths are less than ~0.25 eV in the laboratory frame, corresponding to ~50 meV collision energy resolution

for $B_3O_4^+$ + HF. This represents a >20 fold improvement in mass resolution with no loss of collision energy resolution, compared to our original instrument. To our knowledge, quadrupole mass filters have not been used in this configuration previously, and we will be reporting the details in Review of Scientific Instruments.

IV. Raw Cross Section Results

The experimental results are the cross sections for all product species as a function of collision energy. Cross sections are a microscopic measure of chemical reactivity, and can be converted to macroscopic kinetic parameters by appropriate averaging, as discussed below. Because cross sections reflect the un-averaged collision energy behavior, mechanistic and energetic information can be extracted more directly than from rate measurements.

We have conducted extensive experiments for reactions of $B_nO_m^+$ (n = 1-3, m=1-4) and $B_nO_mH^+$ (n = 1-2, m=1-3) with HF. To provide more information about the energetics and structure of some of the product species, we also did more abbreviated experiments for $BO^+ + D_2$, $BO^+ + D_2O$, $HBO^+ + D_2$, and $HBO^+ + D_2O$. For comparison, cross sections also were measured for B_n^+ + HF and B_nH^+ + HF. Cross Sections are measured for all significant product channels (>0.2 Å^2), at collision energies ranging from 0.1 to 10 eV. The kinetics are most dependent on the low energy data, but the high energy behavior provides us with additional mechanistic insight. This report will focus on those aspects of the results that are relevant to combustion. Full details of the reaction dynamics will be published separately.

A) The $B_nO_m^+$ + HF system:

Figures 1 and 2 present the cross sections for reaction of pure $^{10}B_nO_m^+$ oxide clusters with HF. In our previous results[1], the oxide beam had contamination from both ^{11}B oxide clusters and from $^{10}B_nO_mH^+$. As expected, the old results can be understood as a linear combination of boron oxide and hydrogenated boron oxide chemistry. Fortunately, the $^{10}B_nO_mH^+$ contamination was only a small fraction of the total "oxide" beam intensity, and therefore there are no major problems with the old data for the oxides. We do observe somewhat smaller cross sections in the new experiments, and a few minor products have been reassigned as being at least partially due to reaction of the

hydrogenated oxides.

For the oxides there are several trends to note. For all sizes and stoichiometries the major product channels involve elimination of either FBOH or FBO, in both cases stripping a BO unit from the parent oxide cluster:

$$B_nO_m^+ + HF \rightarrow FBOH^+ + B_{n-1}O_{m-1} \quad (1a)$$

$$\rightarrow FBOH + B_{n-1}O_{m-1}^+ \quad (1b)$$

$$\rightarrow FBO^+ + B_{n-1}O_{m-1}H \quad (2a)$$

$$\rightarrow FBO + B_{n-1}O_{m-1}H^+ \quad (2b)$$

Both reactions occur with no activation energy for all size clusters, as shown by the collision energy dependence of the cross sections. Reaction 1 dominates for every parent oxide cluster studied except $B_3O_4^+$ where reaction 2 is dominant. The branching between 1a and 1b and between 2a and 2b depends on the relative ionization potentials of the two products in each reaction. Evidently, the IPs of FBO and FBOH are similar to those for the boron oxides, though none are known with much certainty. For reaction of BO^+ (Fig.1), the major product channel is formation of $FBO^+ + H$, but this reflects the fact that any $FBOH^+$ formed must decompose in order to conserve energy.

An unusual feature of these cross sections is the sharply peaked collision energy dependence. The reactions are quite efficient at collision energies below a few tenths of an electron volt, but essentially stop above 1 eV. We infer from this that the reactions are strongly dependent on the geometry of the collision, as will be explained below.

In figure 3, we summarize the dependence of total reactivity and product branching (at 0.1 eV collision energy) on reactant cluster size and stoichiometry. Reactivity generally increases with cluster size, suggesting that macroscopic boron oxide surfaces should be quite reactive with HF. Product distributions are not strongly dependent on either size or composition. The chemistry appears to be controlled by elimination of a stable leaving group (BO, FBO, FBOH, BO_2).

Two minor products that provide some insight into the reactant cluster structures are B^+ and BO^+ fragments. These product channels alternate in relative importance with cluster size. The B^+ product is seen for the BO^+, B_2O^+, $B_2O_2^+$, and $B_3O_3^+$ reactant clusters (i.e. sizes where # of O atoms $\leq$ # of B atoms), consistent with linear structures with one end terminated by a boron atom. For example, the proposed structure for $B_2O_2^+$ is $[B\text{-}O\text{-}B{=}O]^+$. For all other clusters (# of O atoms > #

of B atoms), the favorable fragmentation product is loss of BO^+, suggesting that both ends of the cluster are terminated by B=O groups (Using the resonance structure of $B_2O_3^+$ as an example: [O=B-O-B=O]$^+$. This is consistent with structures proposed by Doyle[5].

B) The $HB_nO_m^+$ + HF system

The effects of adding a single hydrogen atom can be seen in the cross sections presented in figures 4 and 5. These data have been corrected for isotope contamination present during the experiment. For example, mass 43 has contributions from both $H^{10}BO_2^+$ and from $^{11}BO_2^+$. Since we also can measure the intensity of the main $^{10}BO_2^+$ peak, and the ^{10}B:^{11}B ratio in our sample (94:6), it is straightforward to correct the $HB_nO_m^+$ signal for ^{11}B contamination. A similar correction can be applied to the products from reaction of $HB_nO_m^+$ since we have separately measured the cross sections for the pure oxides (figures 1 and 2). We used the following formula to extract the true cross sections for the $HB_nO_m^+$ clusters:

$$\sigma_{hydrogenated} = (\sigma_{total} - K_{isotope}\sigma_{isotope})/ K_{hydrogenated}$$

where the σ's are cross sections and the K's are scaling factors that depend upon the fraction of isotope and hydrogenated boron oxide present during the experiment. The only problem with this situation is that the resulting cross sections are noisier than we would like because in many cases the isotope contamination dominates the signal at the masses in question. Since the isotope contamination increases with number of B atoms, we were unable to obtain acceptable data for $B_3O_3H^+$ and $B_3O_4H^+$. We are investigating several approaches to this problem, including producing ^{11}B purified boron oxide and/or deuterium substituting the oxides.

The striking feature of this system is the dramatic decrease in the total reactivity compared to the pure oxide cluster results. This is shown in figure 6, which compares the two systems at 0.1 eV collision energy. Addition of a single hydrogen atom to each of the $B_nO_m^+$ cluster sizes can decrease the reactivity by up to a factor of 10. For the only doubly hydrogenated ($HOBOH^+$) case we were able to study, the reactivity is practically zero at low collision energy. These results provide additional evidence regarding the reaction mechanism and its relationship to the reactant cluster structure, as discussed below.

Although the total reactivity is substantially lowered, the other features of this system parallel

those found in the $B_nO_m^+$ + HF reactions quite closely. Similarities include: (1) unusually sharp collision energy dependance, (2) similar reaction pathways leading to FBOH and HBO elimination, (3) similar alternation in the fragmentation products.

One other point to note: in the boron oxide mass spectrum, HBO^+ and $HOBOH^+$ have the largest relative abundance. These molecules are formed with ~ 5 times the intensity of their unhydrogenated counterparts, suggesting that these are particularly stable species.

C) Reactions with D_2 and D_2O

To gain additional insight into the properties of the B_xO_yH species, we also ran some preliminary studies of their reactions with D_2 and D_2O (figure 7). By using deuterated reactants we can observe H-atom exchange reactions directly.

We find that BO^+ reacts similarly with D_2 and D_2O. The major reaction in both cases is D-atom addition, forming DBO^+, and in both cases this reaction is efficient and proceeds with no activation barrier. In neither case do we see the sharp collision energy dependence observed in the reactions with HF, and there is significant product intensity out to collision energies of 7 eV. (For the D_2O reaction there is a large signal for D_3O^+. This is a secondary reaction product formed by proton transfer from the primary DBO^+ product to the D_2O in the scattering cell).

In contrast to BO^+, HBO^+ reacts quite differently with D_2 and D_2O. The main reaction with D_2 is D-atom abstraction, but it is roughly an order of magnitude less efficient than for BO^+. At high collision energies we also observe B^+, which is rather unexpected.

Reaction of HBO^+ is quite efficient at low collision energies. The dominant reactions are:

$$HBO^+ + D_2O \rightarrow HOBOD^+ + D \quad (3a)$$

$$\rightarrow DOBOD^+ + H \quad (3b)$$

$$\rightarrow HD_2O^+ + BO \quad (4)$$

If reaction 3 (HOBOH formation) proceeded by formation of a long-lived complex followed by H or D elimination, we would expect a 1:2 ratio of the $DOBOD^+$:$HOBOD^+$ products. Instead, we observe 1:4 ratio, implying that a direct reaction mechanism is occurring.

Reaction 4 is proton transfer to water. The fact that this proceeds with no activation barrier

proves that the H^+-BO bond energy is less than 7.2 eV[9]. This number is useful in the thermochemistry discussion given below. We are currently finishing up a more complete set of experiments with the $B_nO_mH_x^+ + D_2O$ system.

D) The B_n^+ + HF system

The left side of figure 8 shows cross sections for reaction of a few different size pure boron cluster ions with HF. The dependence of reactivity on cluster size is summarized in figure 18. In contrast to the situation for the oxides, the chemistry of the pure boron clusters depends strongly on cluster size. The small clusters (B_n^+, n= 1-7, 9) react with no activation barriers and with efficiency ranging from 30 to 50%. For the larger clusters (n = 8, 10-14) reaction occurs only with substantial activation energy and the reactivity is much reduced. The observed collision energy thresholds could either indicate growth of activation barriers for reaction of the larger clusters or that the reactions become endoergic with increasing size.

The type of products formed also changes somewhat. For the small clusters, the dominant reactions are BF and H elimination:

$$B_n^+ + HF \rightarrow B_{n-1}H^+ + BF \quad (5)$$

$$\rightarrow B_nF^+ + H. \quad (6)$$

For intermediate sizes (n = 5, 7, 9) an adduct formation reaction is observed:

$$B_n^+ + HF \rightarrow B_nHF^+ \quad (7)$$

with the adduct decaying primarily by BF elimination at higher collision energies. The existence of the adduct (a metastable collision complex that survives long enough for us to detect it) has important implications for the thermochemistry of the boron-HF system. For adducts to be detected, they must be strongly bound and also have no highly exoergic decay channels. This tends to support that idea that the reaction thresholds observed for the larger clusters are due to real endoergicity, not simply activation barriers.

For the large clusters there is little low energy reactivity and different product branching is observed. The lowest energy channels are BF elimination (reaction 5) and H elimination (reaction 6). At higher energies, a B_{n-1}^+ product is observed. Since this channel turns on at the energy that reaction 5 is turning off, we believe that the primary $B_{n-1}H^+$ product is simply decomposing due to

excessive internal energy.

E) The B_nH^+ + HF system

The right half of figure 8 shows cross sections for reaction of selected mono-hydrogenated boron cluster ions. These experiments were done with ^{11}B enriched boron, thus there is no ambiguity regarding the identity of the m+1 mass peaks. In contrast to the oxides, where mono-hydrogenation results in large decreases in reactivity, addition of hydrogen to pure boron seems to make little difference in either the reactivity or the product distributions. The major reactions include:

$$B_nH^+ + HF \rightarrow B_{n-1}H_2^+ + BF \quad (8)$$

$$\rightarrow B_nF^+ + H_2 \quad (9)$$

Reaction 8 is analogous to reaction 5 in the pure boron clusters, and reaction 9 is analogous to reaction 6, with the exception that H_2 is eliminated, rather than H.

V. Reaction Efficiencies

For use in combustion models, we have converted our cross section data to the equivalent thermal rate parameters. The derivation of the reaction probability per collision with the surface has been described in detail elsewhere[10], only a brief description will be given here. To get the reaction probability per collision as a function of energy P(E), we divide the measured reactive cross section $\sigma_{react}(E)$ by the collision cross section. This is taken to be the ion-dipole capture cross section $\sigma_{capture}(E)$ for low collision energies and the hard sphere cross section at high energies. The result is a reaction probability per collision as a function of collision energy. To obtain reaction probabilities as a function of temperature, we simply convolute the P(E) results with the Maxwell-Boltzmann distribution of collision energies for each temperature of interest.

Reaction probabilities are given for the oxides in figures 9 through 11. Note that for the smaller clusters, the reactivity is low but as the cluster size increases the reaction probability increases to ~50% - 60%. For modeling of oxide surfaces, we recommend use of an average of the data for the largest clusters. We report total reaction probability, and the probabilities for the largest product channel. The rest of the product channels are lumped together for simplicity's sake. The breakdown into individual minor product channels can be obtained from figures 1-3.

For the mono-hydrogenated oxides(figures 12 and 13), the reaction probabilities are considerably lower though the products that form are quite similar to those for the pure oxides. The

reactivity does appear to increase with increasing size, though the size range we have been able to study is quite limited for the $HB_nO_m^+$ species. Our recommendation at present is that the effects of hydrogenation need to be included in the heterogeneous models, we suggest a reaction efficiency of about 10%. We are attempting to generate larger hydrogenated oxides to see if they are more reactive.

Reactions efficiencies for some of the other species studied are given in figures 14-17. Figures 20-22 compare total reaction probabilities for all the species studied.

VI. Oxide Structure and Reaction Mechanism

In thinking about how to use these results in understanding chemistry of boron/boron oxide surfaces, it is useful to understand the reaction mechanism and its relation to the cluster structure. Unfortunately there are many pieces of structural and thermochemical information that are missing or highly suspect. The following scenario is therefore somewhat speculative, and we hope that it may stimulate additional discussion, theoretical work, etc. that could lead to a more definitive mechanism. Here are the considerations leading us to the proposed structure/mechanistic picture:

All the major reactions of both the oxide and hydrogenated oxide clusters produce species such as FBOH and FBO, where a single BO unit is lost from the parent cluster. Doyle's CID experiments also primarily show loss of BO groups.

All the major reactions show an unusually sharp collision energy dependance, falling much faster than the collision cross section as the collision energy is increased. Furthermore, this sharpness becomes more pronounced as the size of the cluster increases. We take this as evidence that reaction of HF with $B_nO_m^+$ or $HB_nO_m^+$ clusters (and with boron oxide surfaces) can occur only at particular reactive sites. If the HF strikes the cluster at the wrong position or orientation, then there is a high activation barrier to reaction. At low collision energies, reaction is efficient because the HF binds molecularly to the reactant cluster. This weak "physisorption" process provides time for the HF to find the correct site and orientation so that reaction can occur. As collision energy is raised, the lifetime of this weakly bound complex rapidly decreases, decreasing the reaction efficiency accordingly.

Addition of a single H atom significantly reduces the reactivity of the small oxide clusters (while having little effect on pure boron clusters). We interpret this to suggest that the H atom occupies or blocks a reactive sites and renders reaction more difficult. For the smallest

oxides, reaction is reduced by a factor of ten or more, while for the larger clusters ($B_2O_2^+$, $B_2O_3^+$), reactivity is only decreased by a factor of ~2 - 3. If our reactive site model is correct, this implies that the larger clusters have more than one reactive site, only one of which is blocked by the H atom.

Based on these considerations, we propose a mechanism something like that shown in the box below. HF attacks preferentially at one terminus. Boron-fluorine bond formation occurs with the boron atom of the terminal BO group, and simultaneously the BO bond attaching the terminal group to the oxide cluster breaks, cleaving off FBO. The hydrogen atom can end up either attached to the FBO

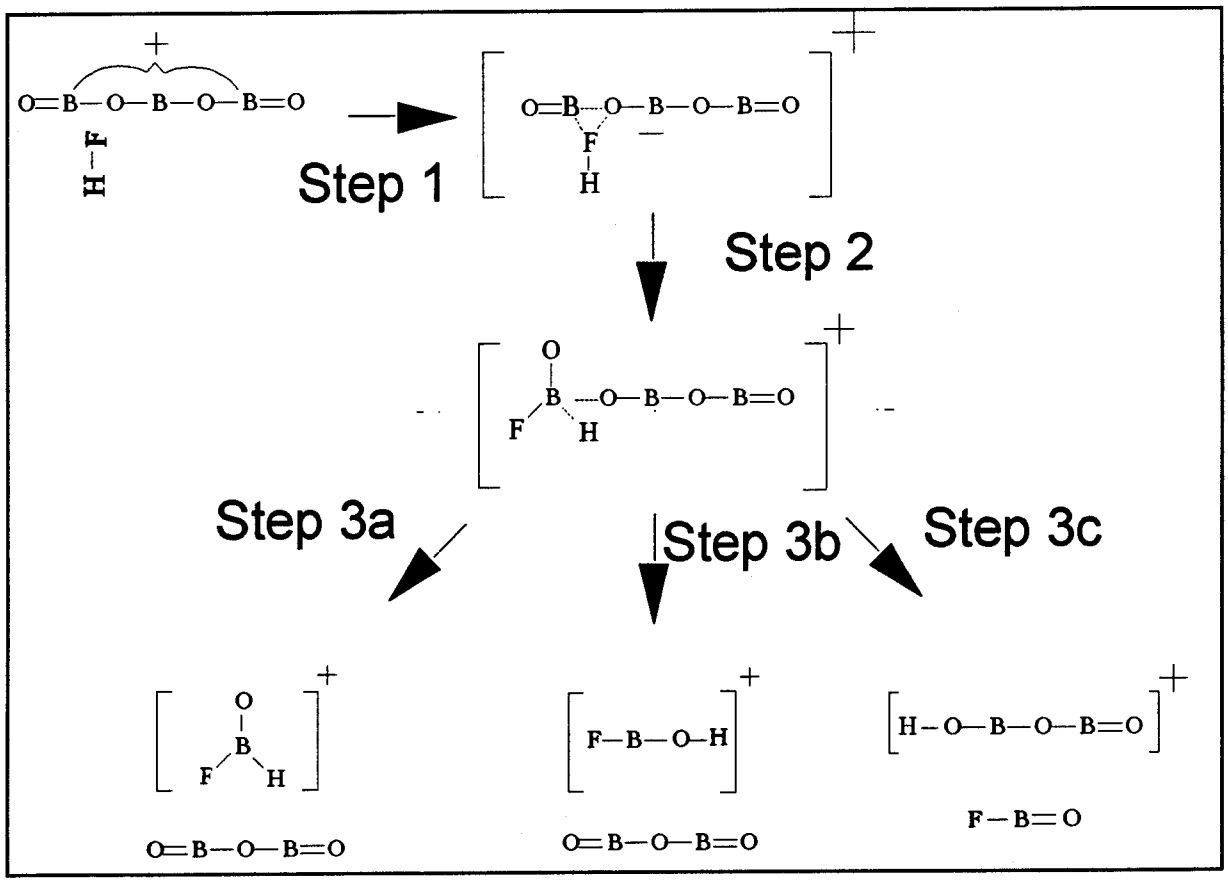

(producing FBOH and $B_{n-1}O_{m-1}$) or to the oxide cluster fragment (producing FBO + $B_{n-1}O_{m-1}$H). These result in reactions 1 and 2 above. The inset illustration depicts the various possibilities schematically. H atoms could block reactivity by bonding to either the B or O atoms of the terminal BO group.

We considered the possibility that the reactive site was an interior B atom (for example the

central atom in the $B_3O_4^+$ shown in the inset. This in principle would be the least coordinatively saturated atom, and therefore the most reactive. The problem with this scheme is how to explain the product distribution, which is overwhelmingly dominated by loss of FBOH or FBO. It is difficult to envision this occurring if the initial B-F bond forms to the central atom.

One problem in proposing mechanisms like this is the lack of information regarding the electronic structure of boron oxides larger than BO. Our understanding about the bonding in these species is left to simple resonance structure arguments. Given the failure of these simple arguments for pure boron clusters, it would not be surprising if the true bonding arrangements were quite different.

VII. Structure and Thermochemistry Problems

The thermochemistry of small H-B-O-F containing molecules is not well developed. For example, FBOH (either ion or neutral) is a major product for oxide-HF reactions, yet the structure and heat of formation are unknown. Soto[11] has calculated the energetics for the reaction of F atoms with HBO, and in the process determined the relative stability of the HB(F)O isomer (see product from step 3a in the above inset). She has not reported the energetics of other isomers, such as linear FBOH, although we understand that these calculations are underway. Our results provide some evidence for the existence of two isomers. In addition to the dominant low energy component, our FBOH cross sections also have a small (0.2 to 1 $Å^2$) component that persists to high energies and which appears in some cases to have a threshold.

There are other thermochemical problems as well. For example, we could estimate energetics for many of the reactions discussed, and for their neutral analogs. In order to do this we need ionization potentials for BO, HBO, FBO, and FBOH. At present the only IPs available for these species are Koopman's theorem results. Koopman's theorem states that the IP for a molecule is simply equal to the energy of the highest occupied molecular orbital. This essentially makes the assumption that the rest of the electrons do not rearrange themselves in response to removing one electron. For most, if not all, of these molecules, this is clearly a bad assumption. For example, using the reported IP for BO (13.0 eV)[9] in a simple thermochemical cycle, one finds that the bond energy of BO is predicted to drop from 8.28 eV to only 3.6 eV[12] for BO^+. This clearly could only happen if there is a large rearrangement of the bonding electrons, thus invalidating Koopman's theorem for this system. Further discussion of this problem can be found in our paper on the boron-water

reaction[12]. Additional theoretical work on small H-B-O-F containing molecules, including true IPs, would be most helpful.

VIII. Conclusions and Recommendations for Modeling

Our main conclusions are:

1) Boron oxide - HF reactions lead mostly to FBO or FBOH elimination.

2) At combustion temperatures, the total reaction efficiencies per surface collision approach ~60% for the larger oxide clusters. This is what we recommend for input to modeling.

3) All major product channels proceed without any significant activation barriers and involve a stable leaving group (BO, BO_2, FBO, FBOH, etc.).

4) We have found that mono-hydrogenation significantly reduces the reactivity of these small oxide cluster ions. We propose that this is due to blocking of reactive sites, and for macroscopic oxides the parameter of interest will be the H surface coverage. Another unknown factor in this context is the stability of the hydrogenated surface. For example, if upon heating, the surface loses hydrogen as HBO, then the hydrogen coverage will not be a significant bottleneck in the combustion process.

5) Our results support Doyle's proposed structures: clusters are comprised of alternating boron oxygen bonds with terminal B=O groups. For ($B_nO_m^+$) m>n clusters, both ends of the cluster will be terminated with B=O groups. For m≤n, one end will be terminated with a bare boron cluster.

6) H atom addition to pure boron cluster ions (B_n^+) does not lead to a reduction in reactivity, presumably because there are a multitude of reactive sites.

7) The prevalence of FBOH in the products suggests that it is a very stable molecule. Our results show some evidence for production of two different FBOH isomers.

8) We have preliminary results for the D_2O / boron oxide reaction. We find much of the chemistry is similar to the HF system, as might be expected since HF and H_2O are isoelectronic. The collision energy dependance is much different, decaying much slower than the HF system.

REFERENCES

1.S.L. Anderson, ONR Report on Preliminary Boron Oxide Results, 1993

2.G.E. Gurr, P.W. Montgomery, C.D. Knutson, and B.T. Gorres, Acta. Cryst. **B26**, 906 (1970).

3.G.E. Jellison, Jr., L.W. Panek, P.J. Bray, and G.B. Rouse, Jr., J. Chem. Phys. **66(2)**, 802 (1977).

4.M. Miyake, T. Suzuki, H. Morikawa, Y. Takagi, and F. Marumo, J. Chem. Soc. Faraday Trans. 1 **80**, 1925 (1984).

5.R.J. Doyle, Jr., J. Am. Chem. Soc. **110(13)**, 4120 (1988).

6.R.J. Doyle, Jr., Anal. Chem. **59**, 537 (1987).

7.L. Hanley, S. A. Ruatta, and S. L. Anderson, J. Chem. Phys. **87**, 260 (1987).

8.L. Hanley, J. L. Whitten, and S. L. Anderson, J. Phys. Chem. **92**, 5803 (1988).

9.S. G. Lias, J. E. Bartmess, J. F. Liebman, J. L. Holmes, and R. D. Levin, J. Phys. Chem. Ref. Data **17**, suppl. 1 (1988).

10.S.L. Anderson, ONR Report on Kinetic Parameters for Boron-HF and Boron-BF3, 1993

11.M.R. Soto, private communication.

12.P. Hintz, S. A. Ruatta, and S. L. Anderson, J. Chem. Phys. **92**, 292 (1990).

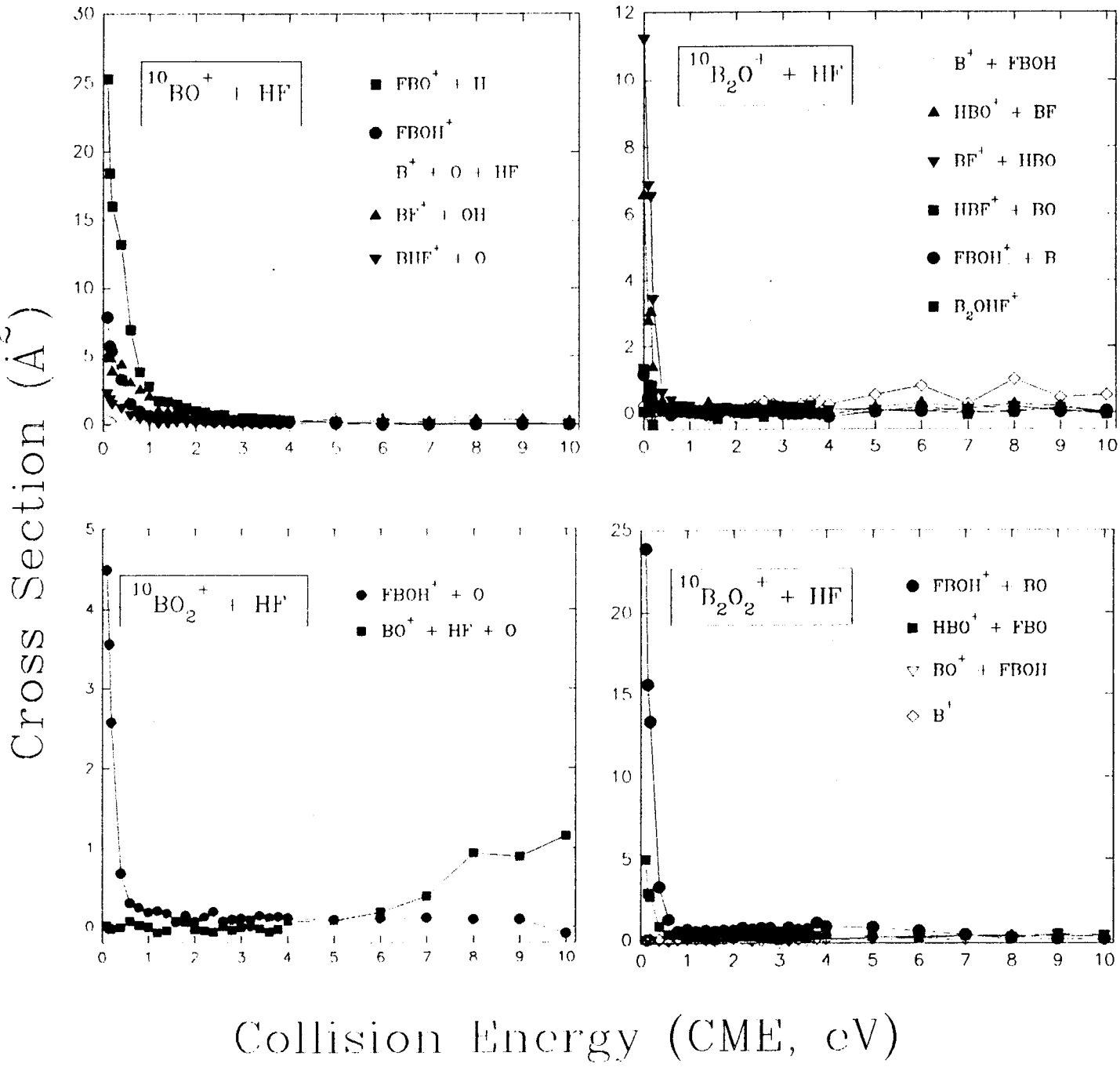
Cross Section (Å^2)
$^{10}BO^+$ + HF
FBO$^+$ + H
FBOH$^+$
B$^+$ + O + HF
BF$^+$ + OH
BHF$^+$ + O
$^{10}B_2O^+$ + HF
B$^+$ + FBOH
HBO$^+$ + BF
BF$^+$ + HBO
HBF$^+$ + BO
FBOH$^+$ + B
B_2OHF^+
$^{10}BO_2^+$ + HF
FBOH$^+$ + O
BO$^+$ + HF + O
$^{10}B_2O_2^+$ + HF
FBOH$^+$ + BO
HBO$^+$ + FBO
BO$^+$ + FBOH
B$^+$
Collision Energy (CME, eV)

Fig.1

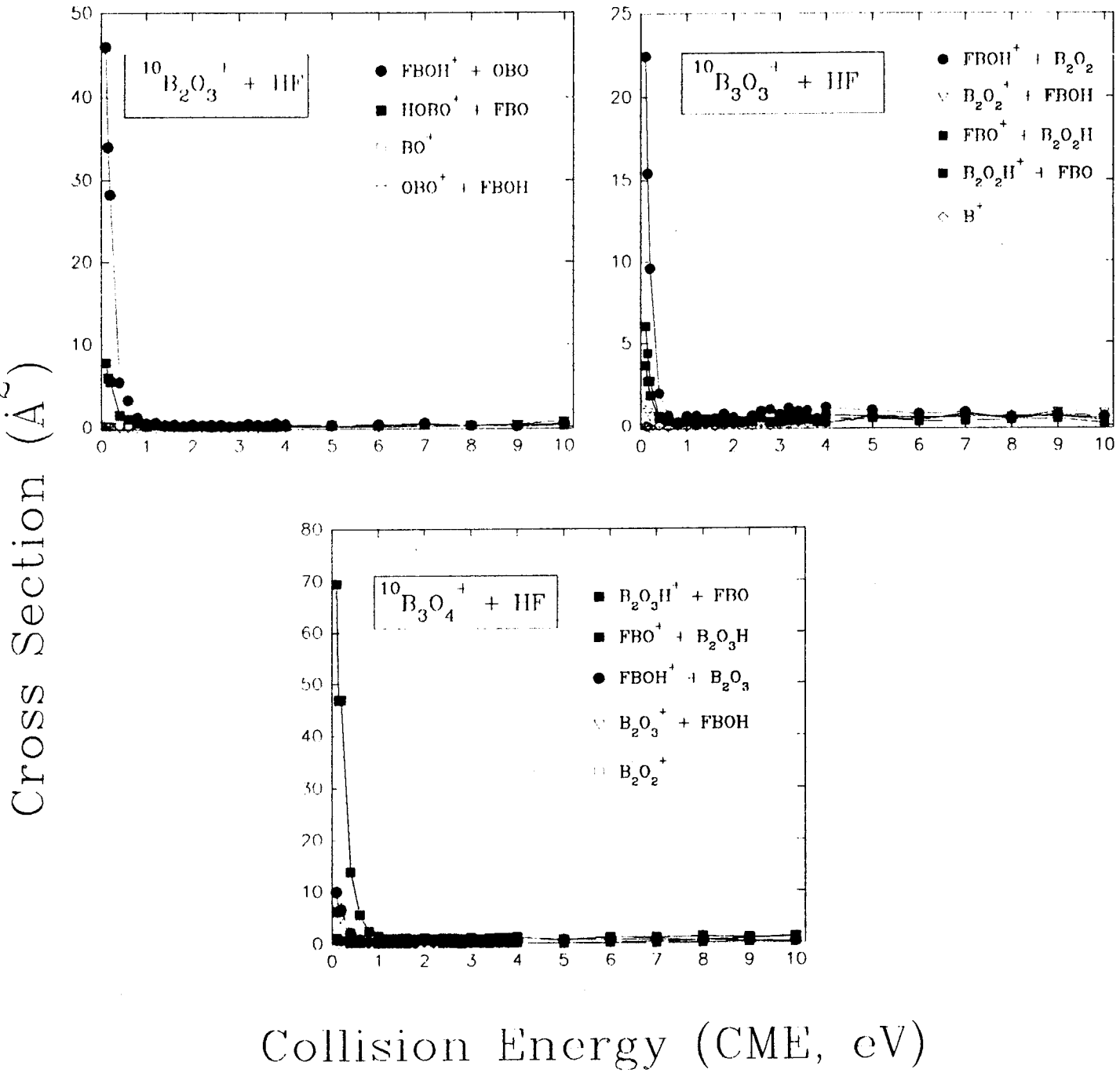
Cross Section ($Å^2$)
$^{10}B_2O_3^+$ + HF
FBOH$^+$ + OBO
HOBO$^+$ + FBO
BO$^+$
OBO$^+$ + FBOH
$^{10}B_3O_3^+$ + HF
FBOH$^+$ + B_2O_2
$B_2O_2^+$ + FBOH
FBO$^+$ + B_2O_2H
$B_2O_2H^+$ + FBO
B$^+$
$^{10}B_3O_4^+$ + HF
$B_2O_3H^+$ + FBO
FBO$^+$ + B_2O_3H
FBOH$^+$ + B_2O_3
$B_2O_3^+$ + FBOH
$B_2O_2^+$
Collision Energy (CME, eV)

Fig.2

Size Dependence of Boron Oxide Clusters at 0.1 eV

$^{10}B_nO_m^+ + HF$

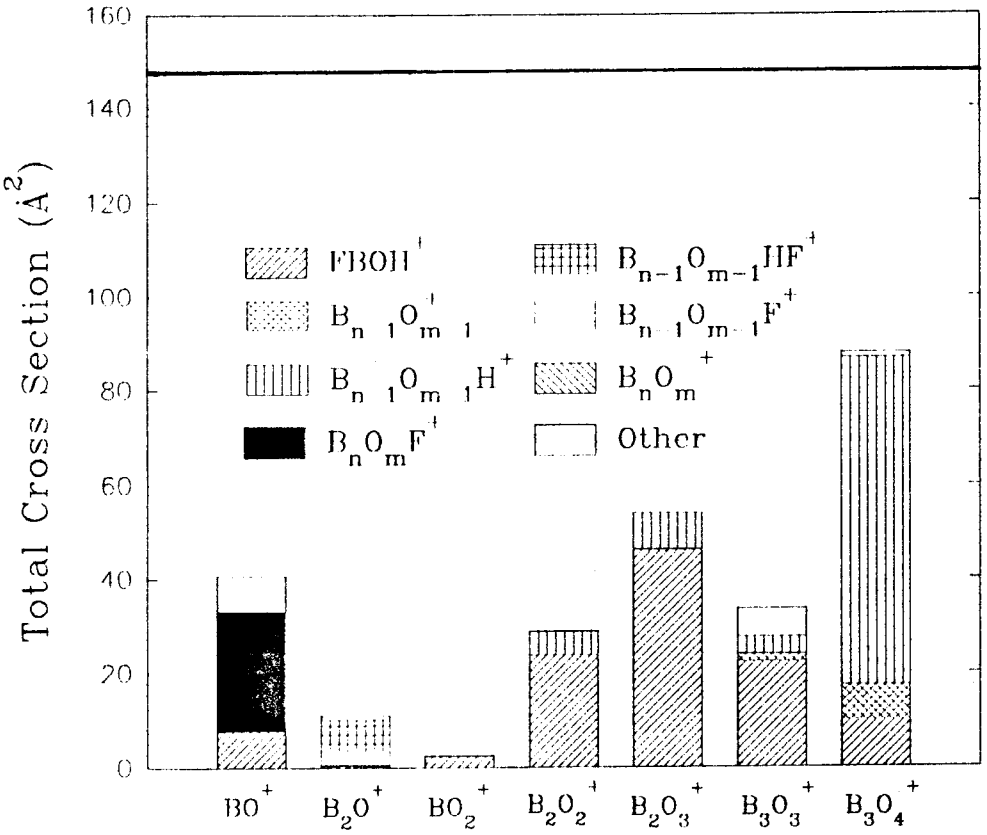

Magnitude of the ion-dipole capture cross section

Fig. 3

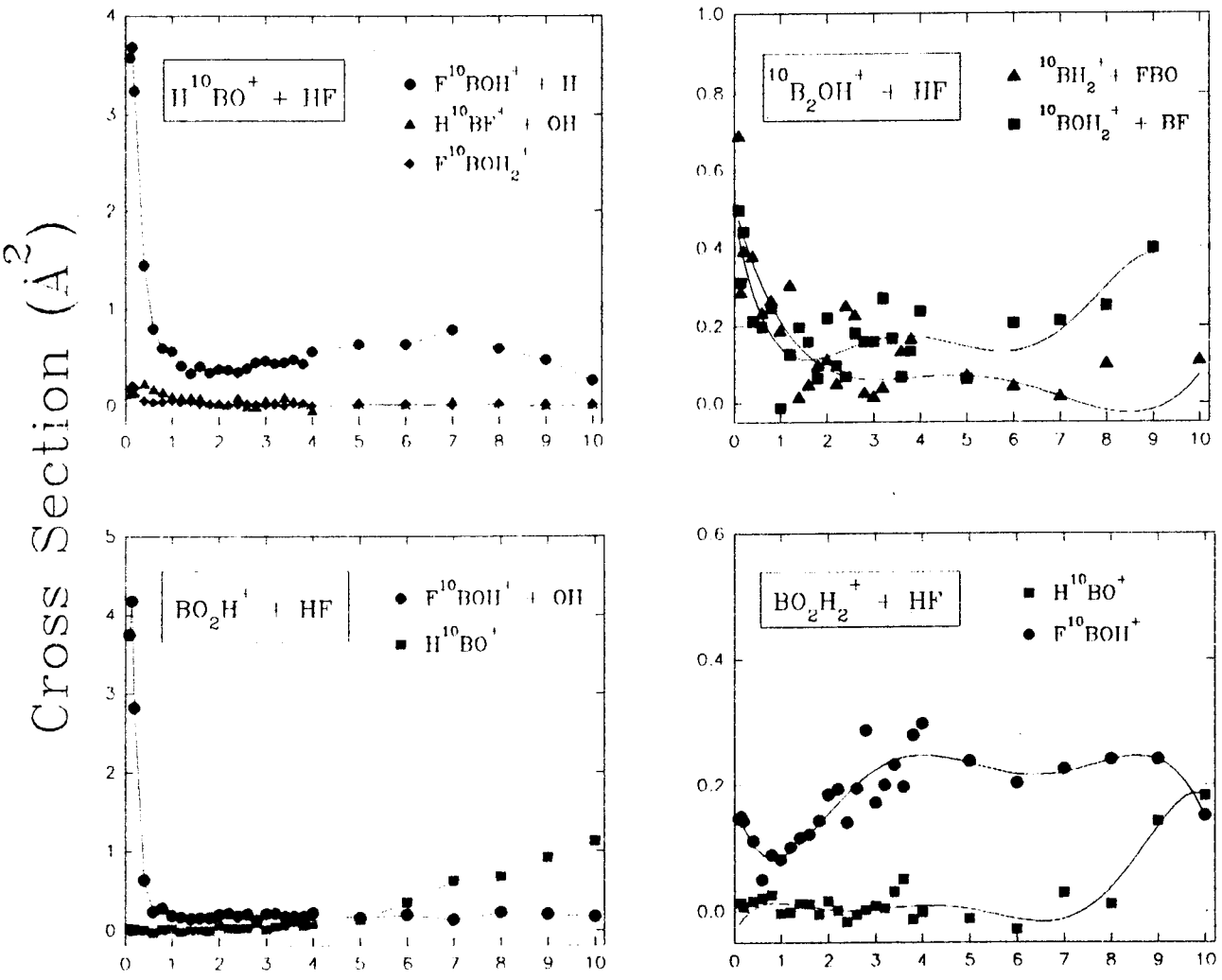
Cross Section (Å²)
H¹⁰BO⁺ + HF
F¹⁰BOH⁺ + H
H¹⁰BF⁺ + OH
F¹⁰BOH₂⁺
¹⁰B₂OH⁺ + HF
¹⁰BH₂⁺ + FBO
¹⁰BOH₂⁺ + BF
BO₂H⁺ + HF
F¹⁰BOH⁺ + OH
H¹⁰BO⁺
BO₂H₂⁺ + HF
H¹⁰BO⁺
F¹⁰BOH⁺
Collision Energy (CME, eV)

Fig. 4

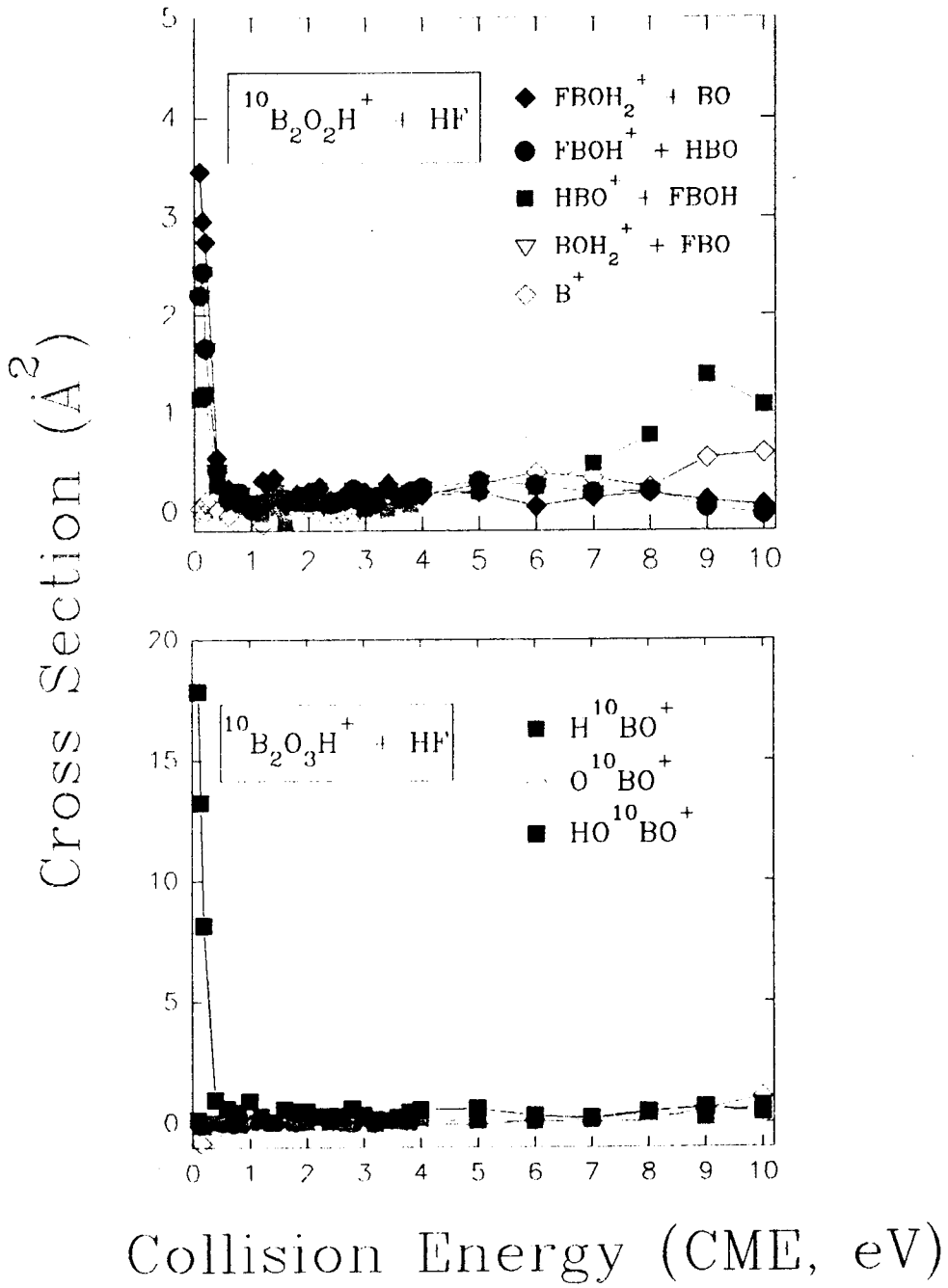
Cross Section ($Å^2$)
$^{10}B_2O_2H^+$ + HF
$FBOH_2^+$ + BO
$FBOH^+$ + HBO
HBO^+ + FBOH
BOH_2^+ + FBO
B^+
$^{10}B_2O_3H^+$ + HF
$H^{10}BO^+$
$O^{10}BO^+$
$HO^{10}BO^+$
Collision Energy (CME, eV)

Fig.5

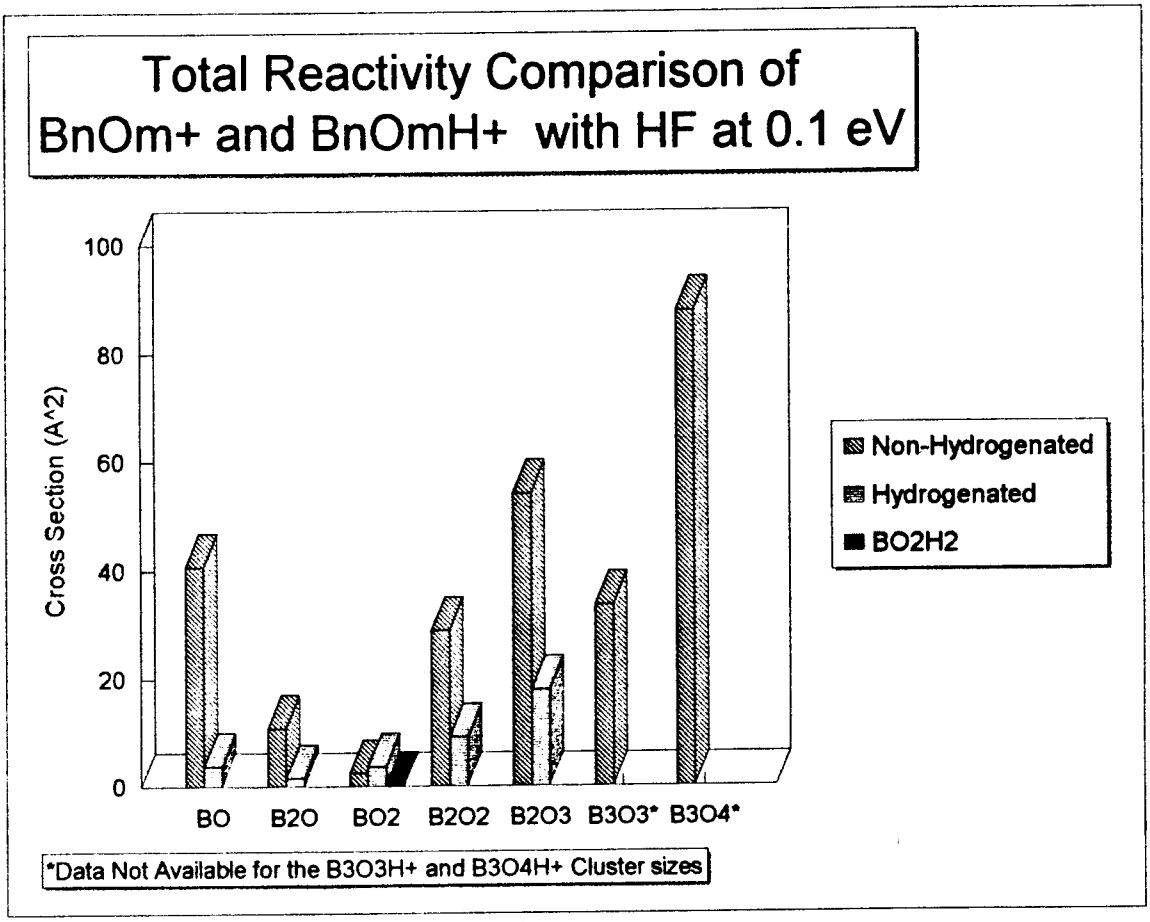
Total Reactivity Comparison of BnOm+ and BnOmH+ with HF at 0.1 eV
Cross Section (A^2)
100
80
60
40
20
0
BO
B2O
BO2
B2O2
B2O3
B3O3*
B3O4*
Non-Hydrogenated
Hydrogenated
BO2H2
*Data Not Available for the B3O3H+ and B3O4H+ Cluster sizes

Fig.6

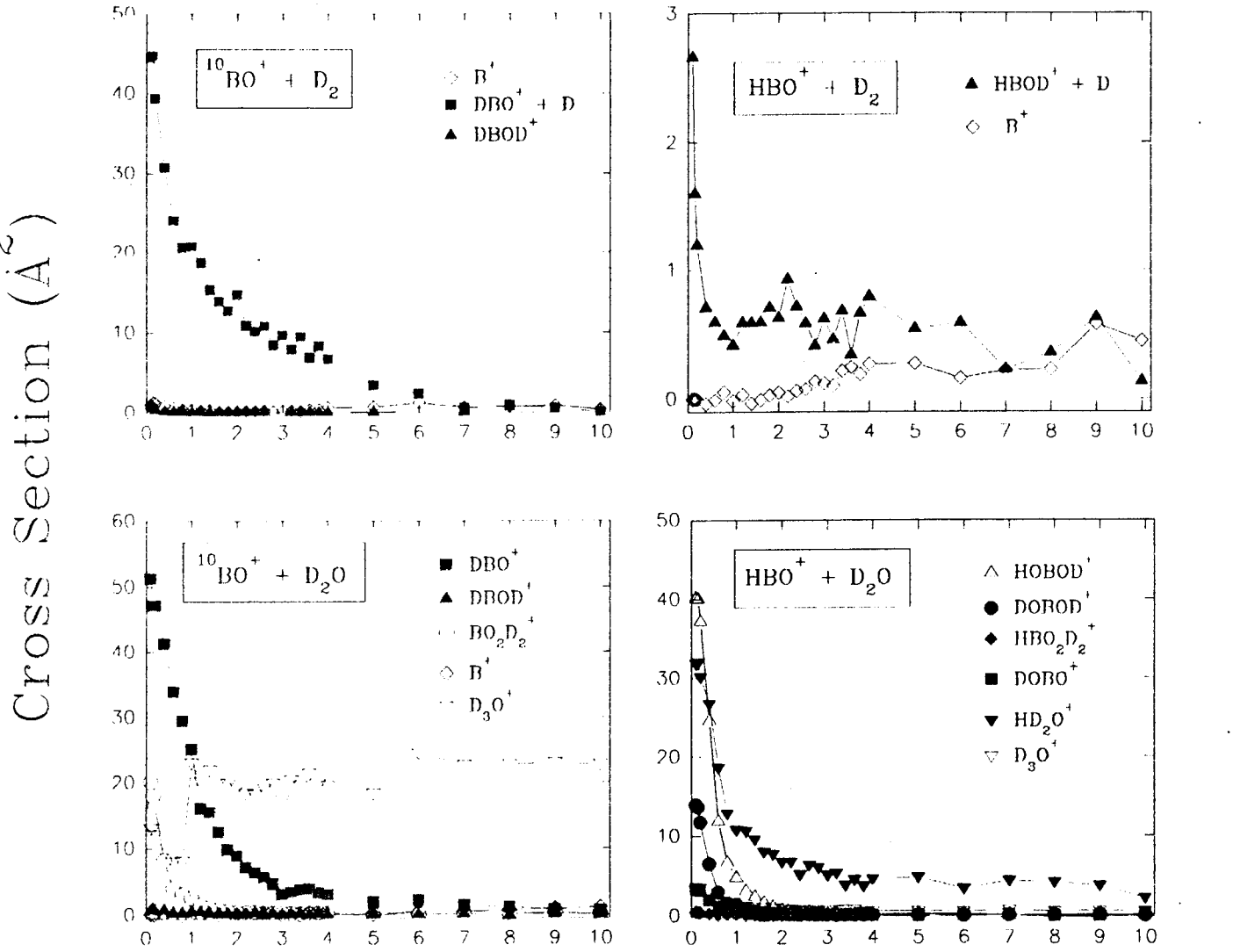
Cross Section (Å^2)
$^{10}BO^+ + D_2$
B^+
$DBO^+ + D$
$DBOD^+$
$HBO^+ + D_2$
$HBOD^+ + D$
B^+
$^{10}BO^+ + D_2O$
DBO^+
$DBOD^+$
$BO_2D_2^+$
B^+
D_3O^+
$HBO^+ + D_2O$
$HOBOD^+$
$DOBOD^+$
$HBO_2D_2^+$
$DOBO^+$
HD_2O^+
D_3O^+
Collision Energy (CME, eV)

Fig.7

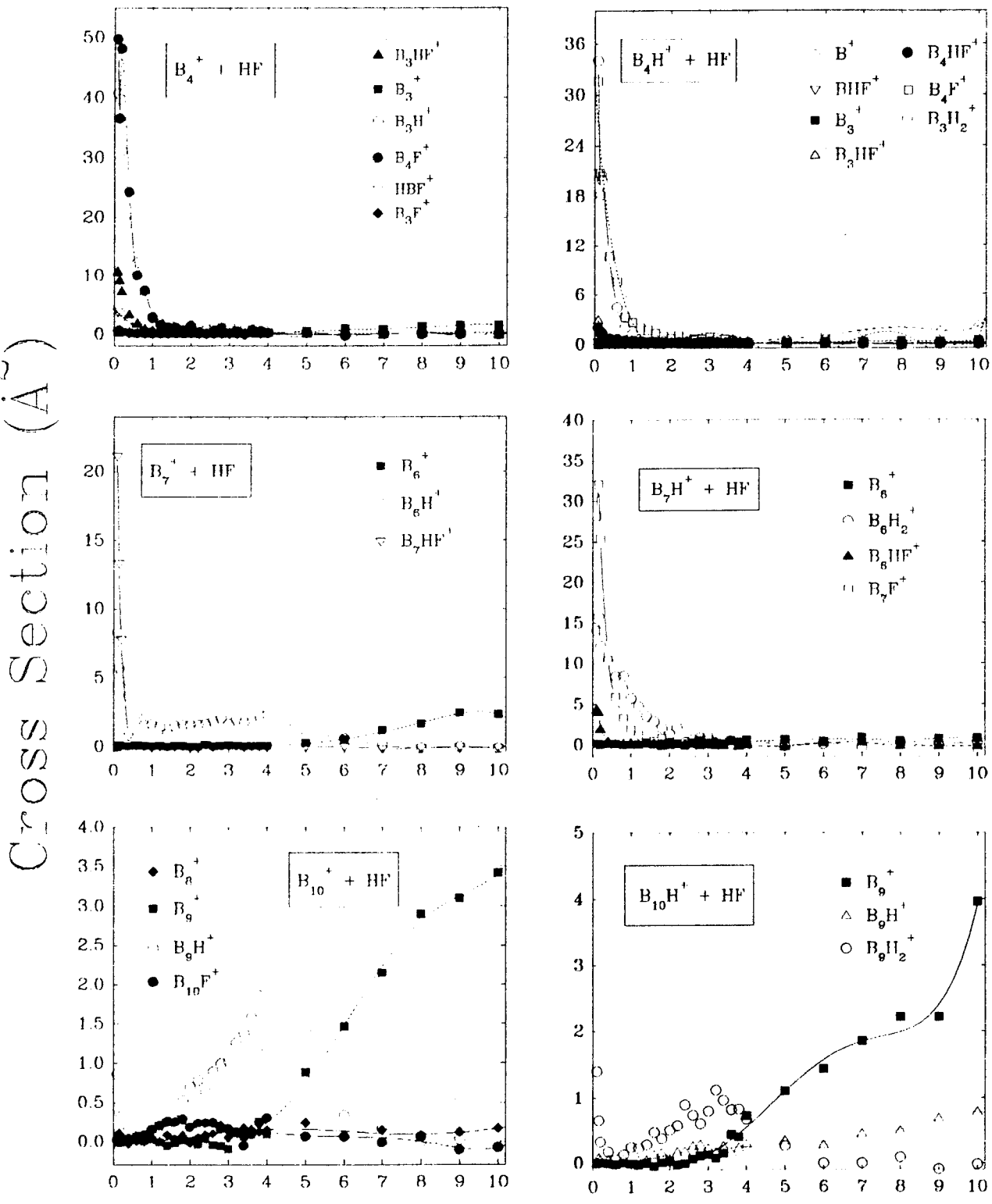
Cross Section (Å²)
B4+ + HF
B3HF+
B3+
B3H+
B4F+
HBF+
B3F+
B4H+ + HF
B+
B4HF+
BHF+
B4F+
B3+
B3H2+
B3HF+
B7+ + HF
B6+
B6H+
B7HF+
B7H+ + HF
B6+
B6H2+
B6HF+
B7F+
B10+ + HF
B8+
B9+
B9H+
B10F+
B10H+ + HF
B9+
B9H+
B9H2+
Collision Energy (CME, eV)

Fig.8

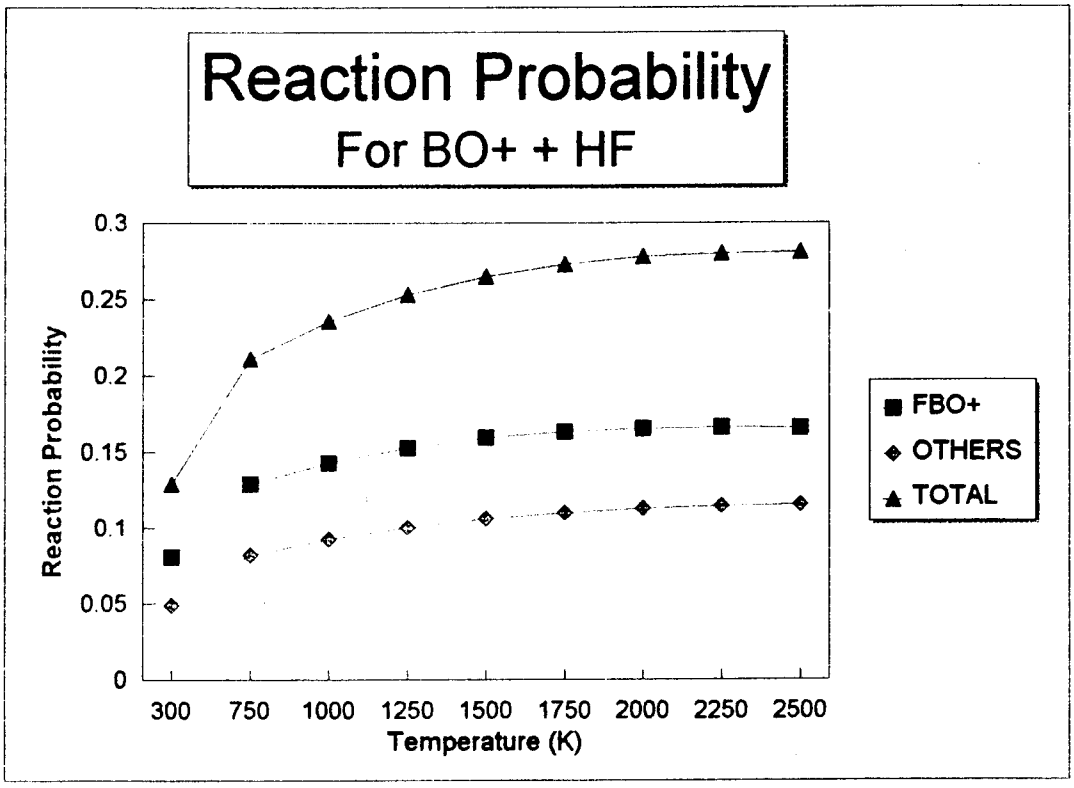
Reaction Probability
For BO+ + HF
Reaction Probability
0.3
0.25
0.2
0.15
0.1
0.05
0
300
750
1000
1250
1500
1750
2000
2250
2500
Temperature (K)
FBO+
OTHERS
TOTAL

Fig.9

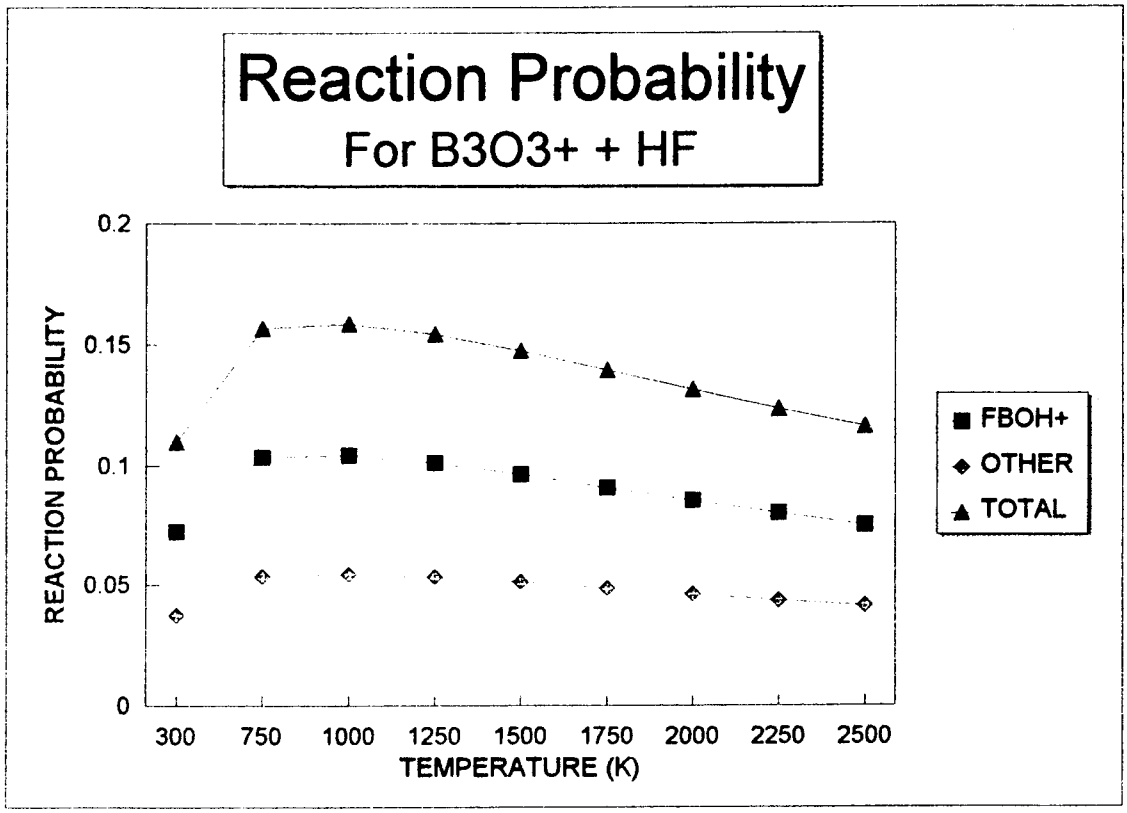
Reaction Probability
For B3O3+ + HF
REACTION PROBABILITY
0.2
0.15
0.1
0.05
0
300
750
1000
1250
1500
1750
2000
2250
2500
TEMPERATURE (K)
FBOH+
OTHER
TOTAL

Fig.10

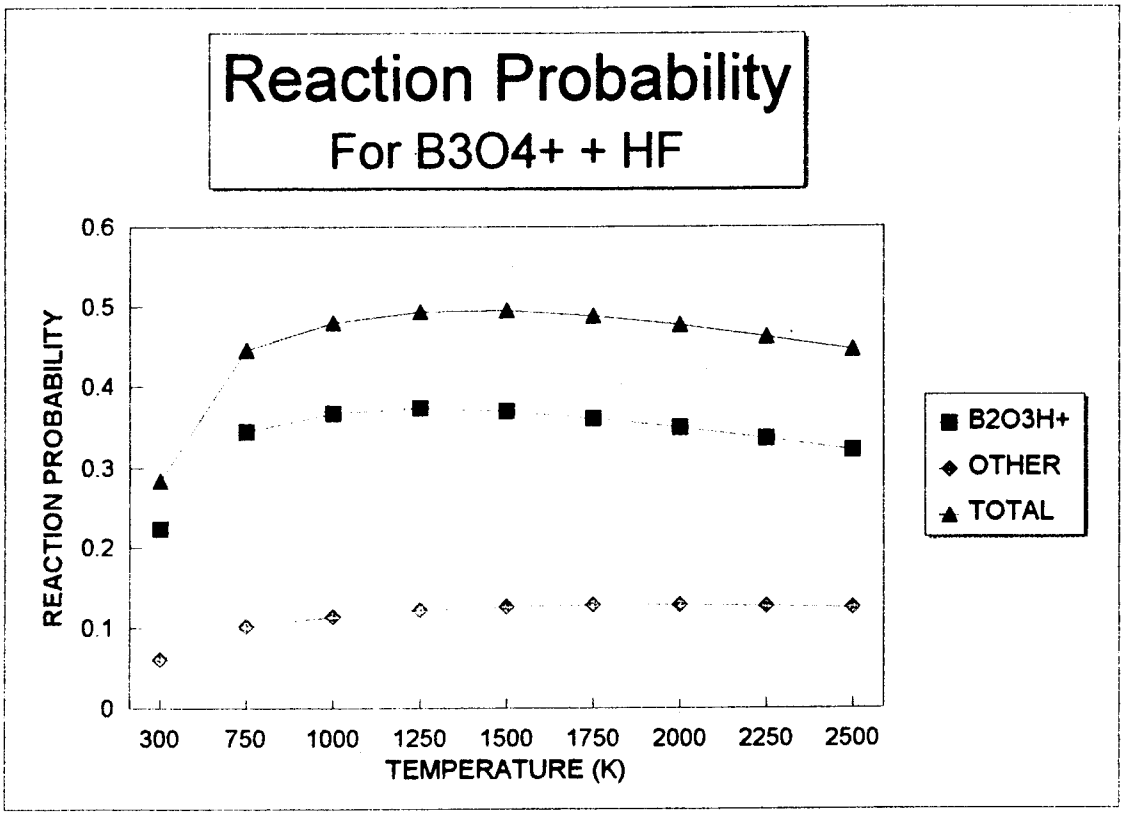
Reaction Probability
For B3O4+ + HF
REACTION PROBABILITY
0.6
0.5
0.4
0.3
0.2
0.1
0
300
750
1000
1250
1500
1750
2000
2250
2500
TEMPERATURE (K)
B2O3H+
OTHER
TOTAL

Fig.11

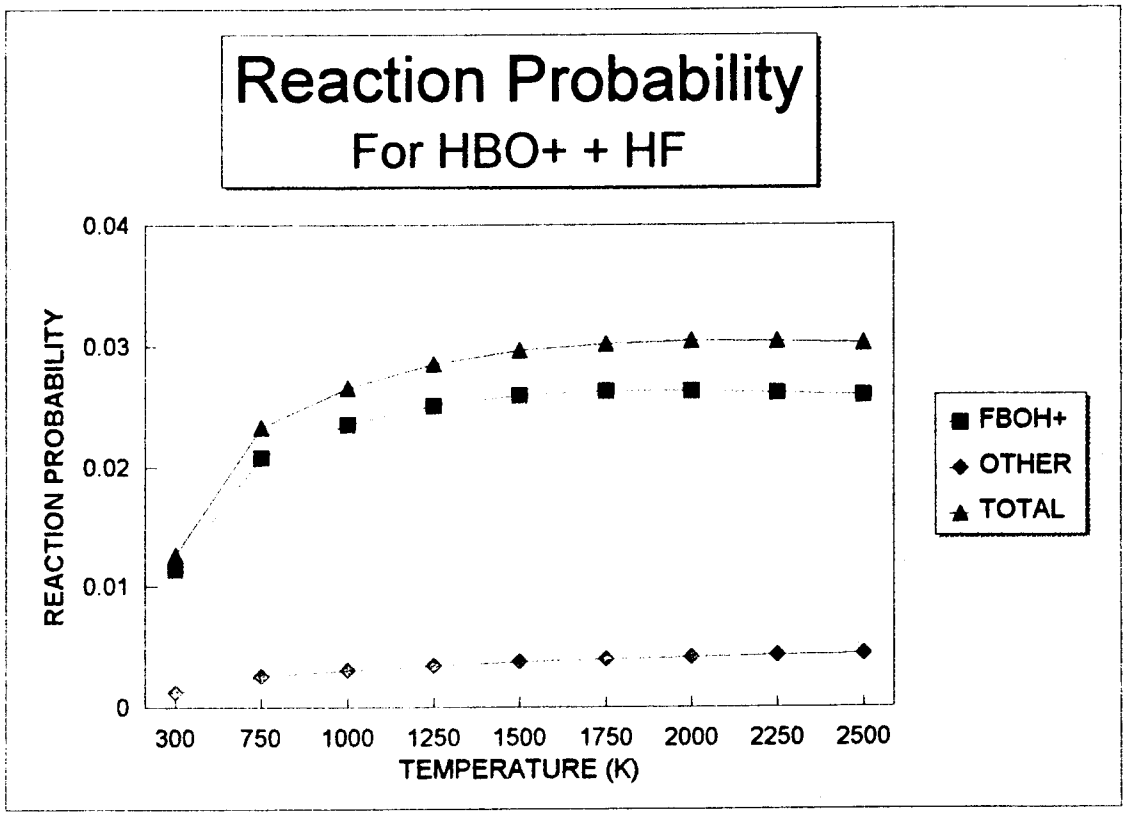
Reaction Probability
For HBO+ + HF
REACTION PROBABILITY
0.04
0.03
0.02
0.01
0
300
750
1000
1250
1500
1750
2000
2250
2500
TEMPERATURE (K)
FBOH+
OTHER
TOTAL

Fig.12

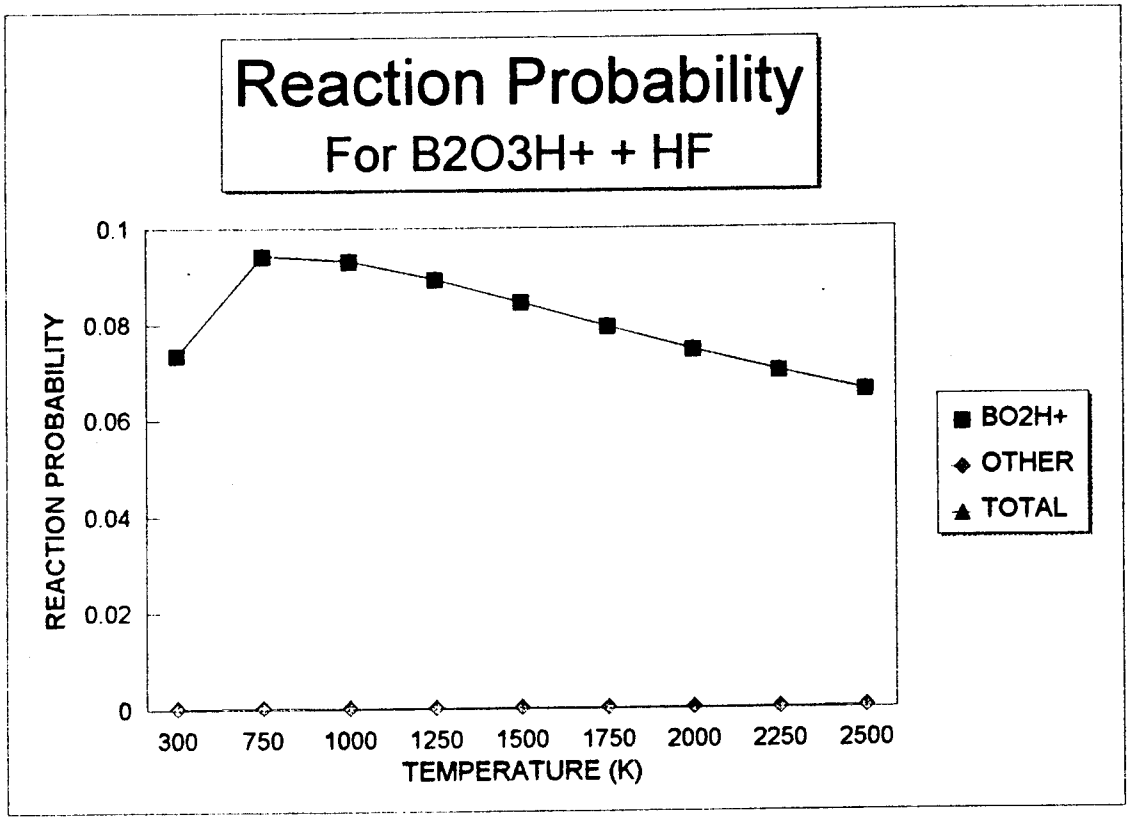
Reaction Probability
For B2O3H+ + HF
REACTION PROBABILITY
0.1
0.08
0.06
0.04
0.02
0
300
750
1000
1250
1500
1750
2000
2250
2500
TEMPERATURE (K)
BO2H+
OTHER
TOTAL

Fig.13

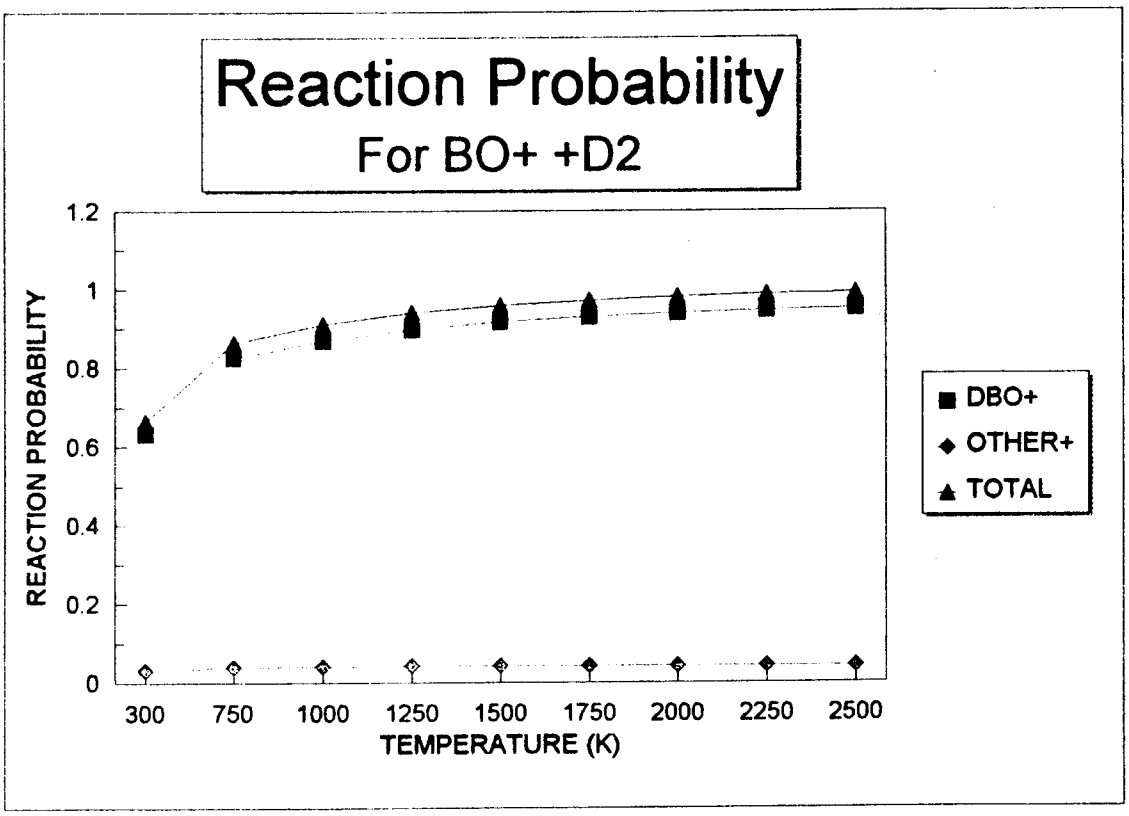
Reaction Probability
For BO+ +D2
REACTION PROBABILITY
1.2
1
0.8
0.6
0.4
0.2
0
300
750
1000
1250
1500
1750
2000
2250
2500
TEMPERATURE (K)
DBO+
OTHER+
TOTAL

Fig.14

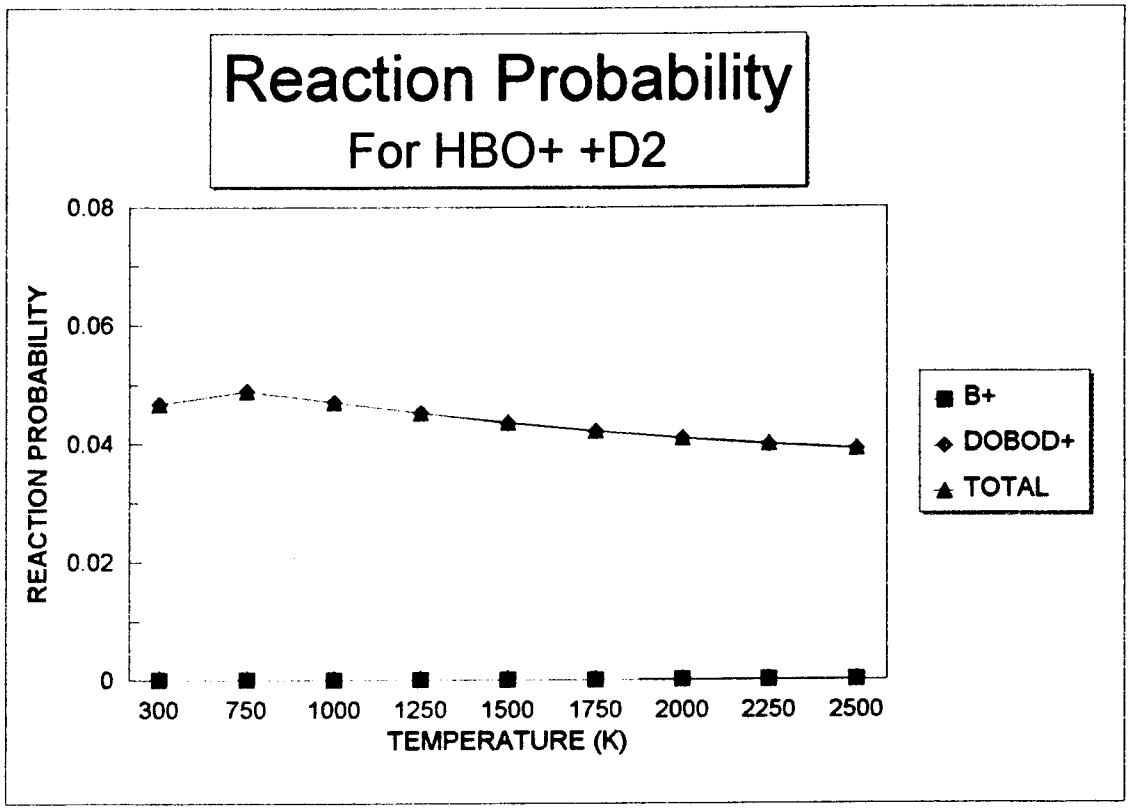
Reaction Probability
For HBO+ +D2
REACTION PROBABILITY
0.08
0.06
0.04
0.02
0
300
750
1000
1250
1500
1750
2000
2250
2500
TEMPERATURE (K)
B+
DOBOD+
TOTAL

Fig.15

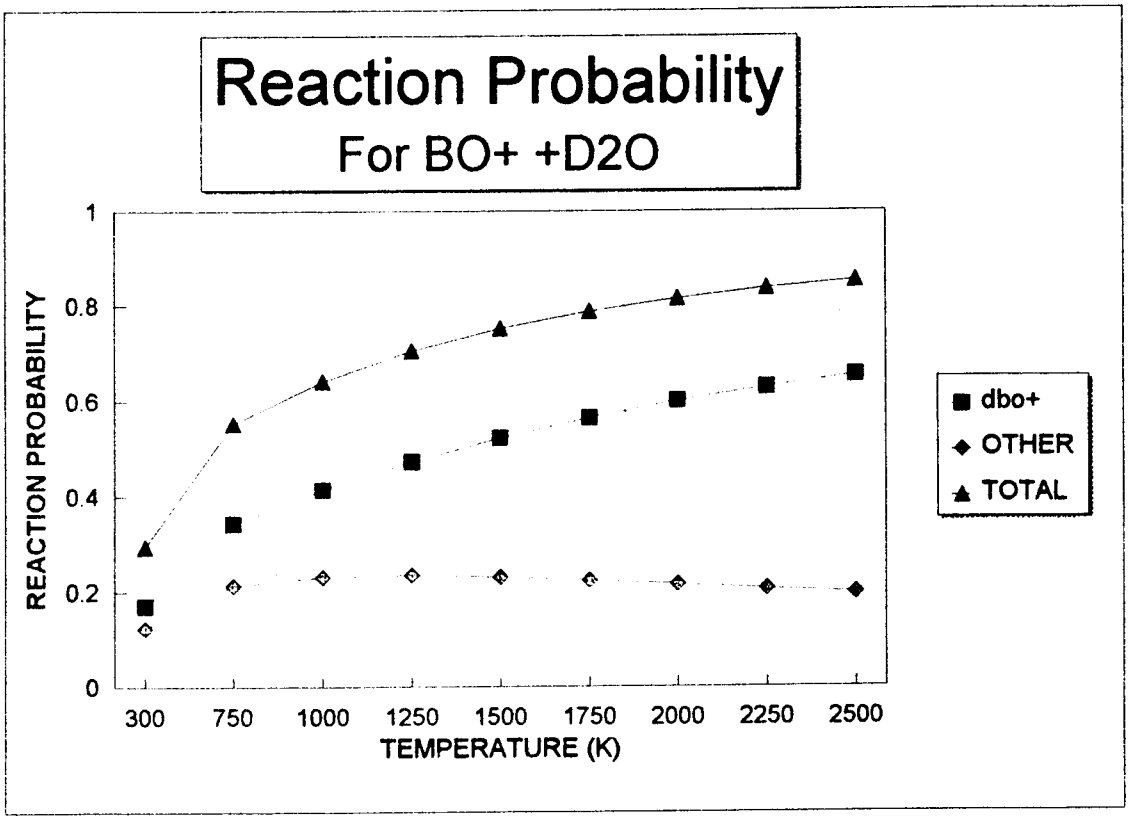
Reaction Probability
For BO+ +D2O
REACTION PROBABILITY
1
0.8
0.6
0.4
0.2
0
300
750
1000
1250
1500
1750
2000
2250
2500
TEMPERATURE (K)
dbo+
OTHER
TOTAL

Fig.16

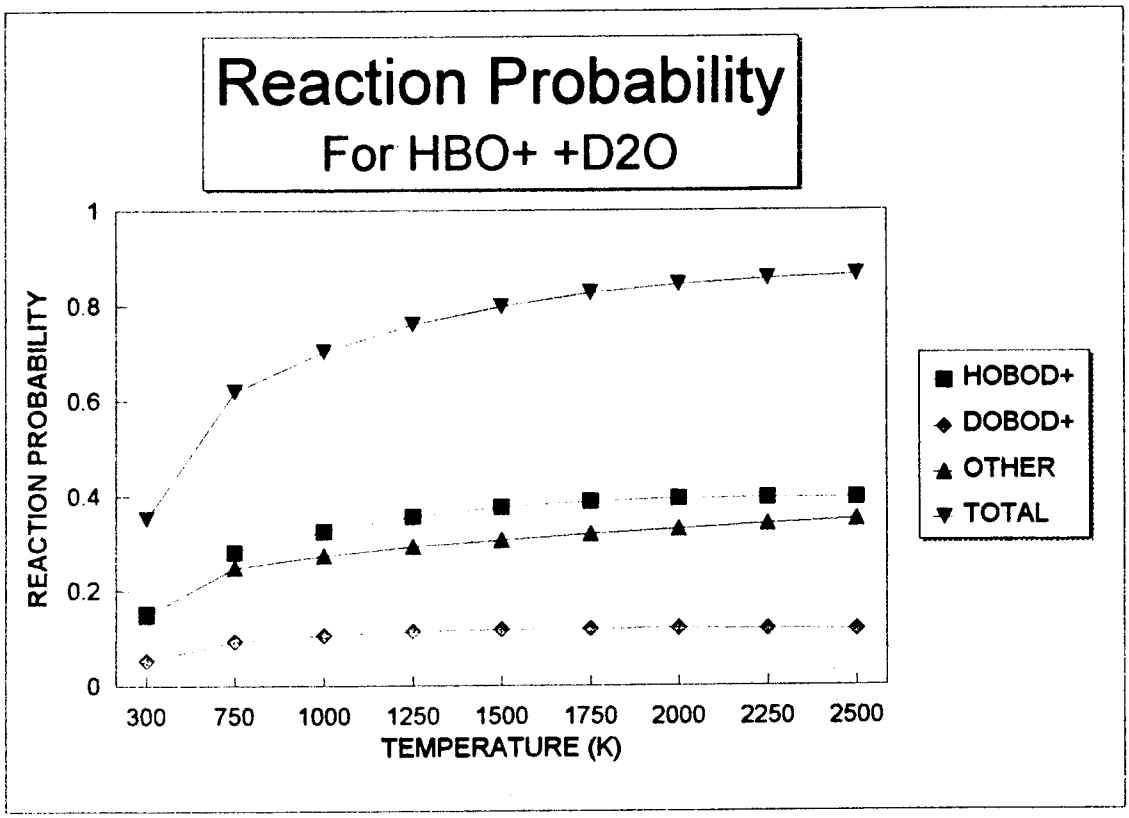
Reaction Probability
For HBO+ +D2O
REACTION PROBABILITY
1
0.8
0.6
0.4
0.2
0
300
750
1000
1250
1500
1750
2000
2250
2500
TEMPERATURE (K)
HOBOD+
DOBOD+
OTHER
TOTAL

Fig.17

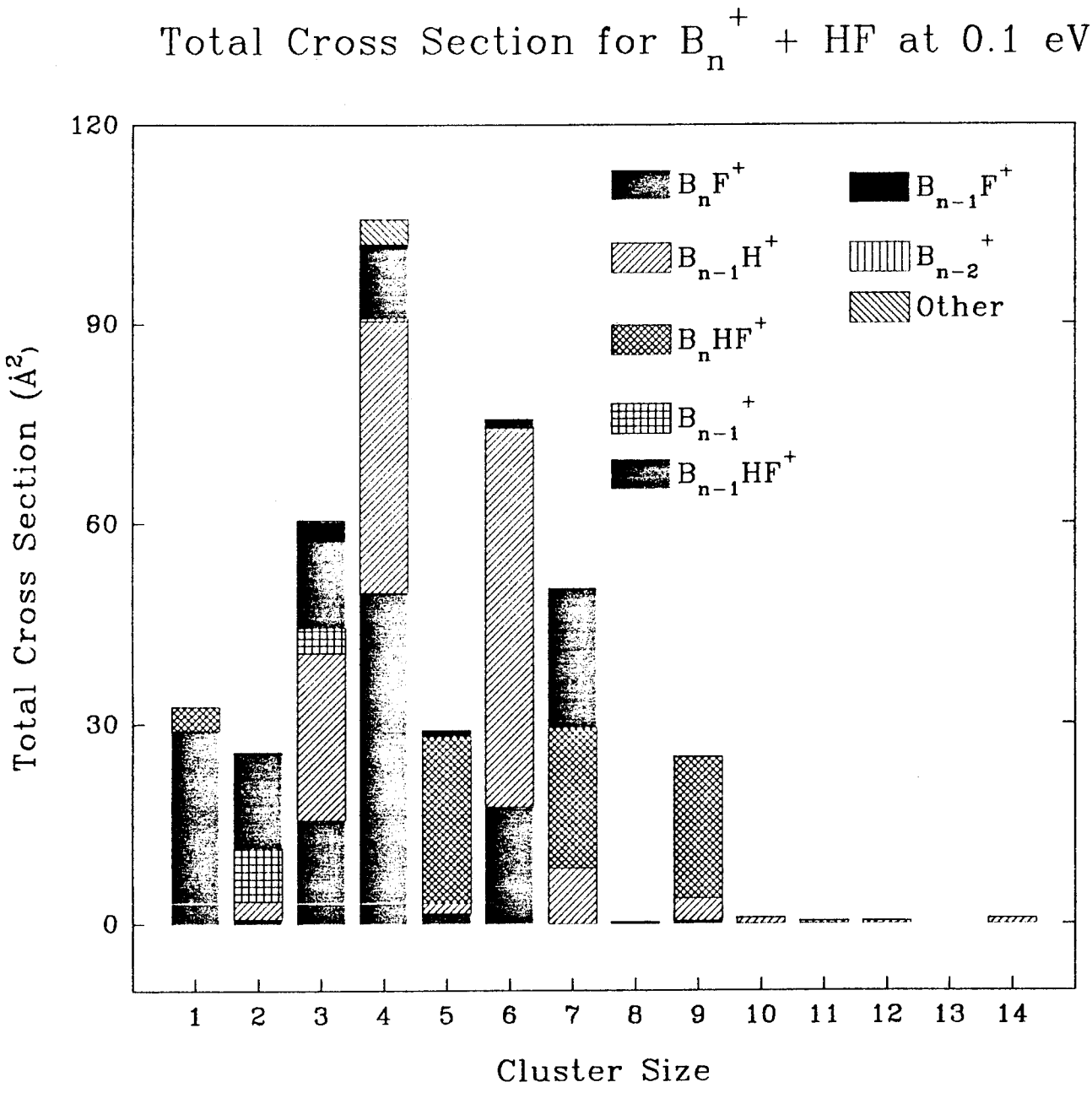
Total Cross Section for B_n^+ + HF at 0.1 eV
Total Cross Section ($Å^2$)
120
90
60
30
0
1
2
3
4
5
6
7
8
9
10
11
12
13
14
Cluster Size
B_nF^+
$B_{n-1}F^+$
$B_{n-1}H^+$
B_{n-2}^+
Other
B_nHF^+
B_{n-1}^+
$B_{n-1}HF^+$

Fig.18

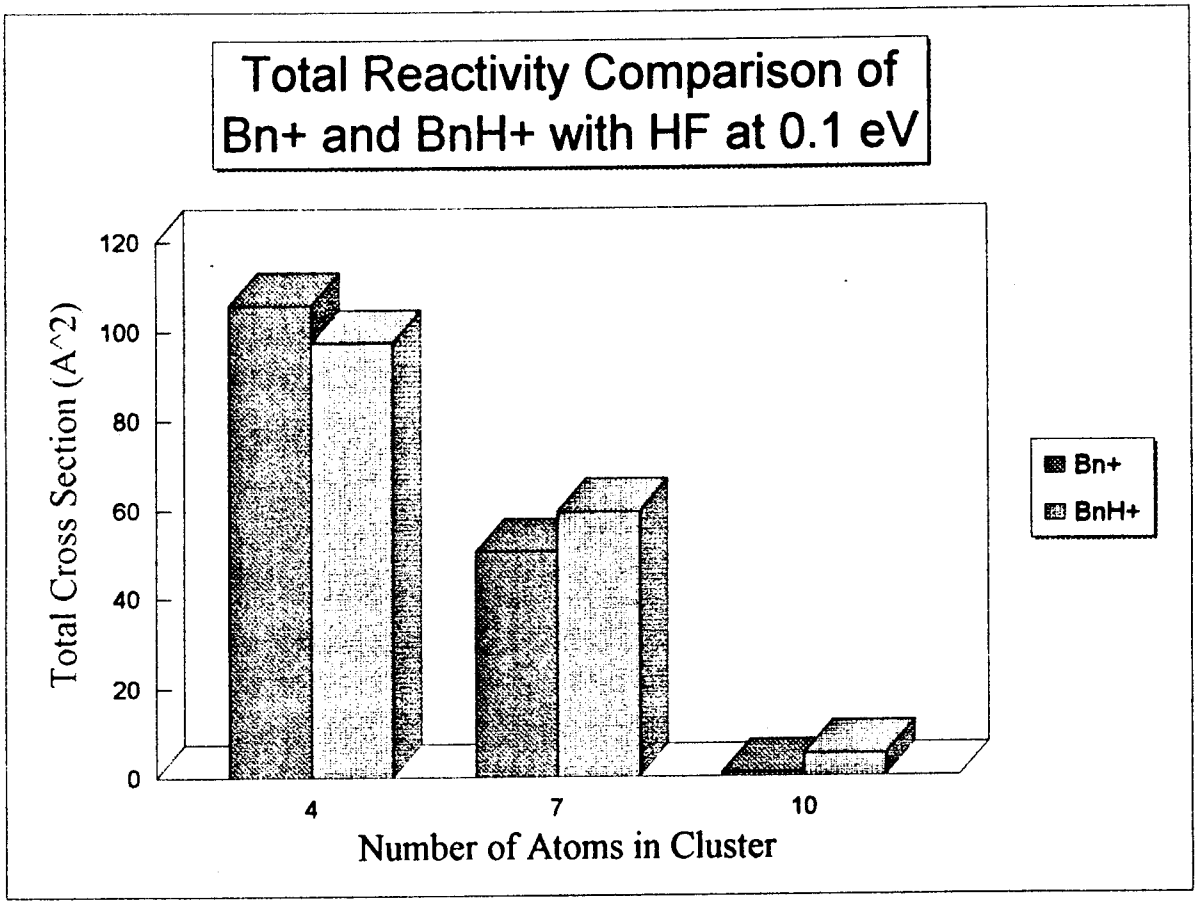
Total Reactivity Comparison of Bn+ and BnH+ with HF at 0.1 eV
Total Cross Section (A^2)
120
100
80
60
40
20
0
4
7
10
Number of Atoms in Cluster
Bn+
BnH+

Fig.19

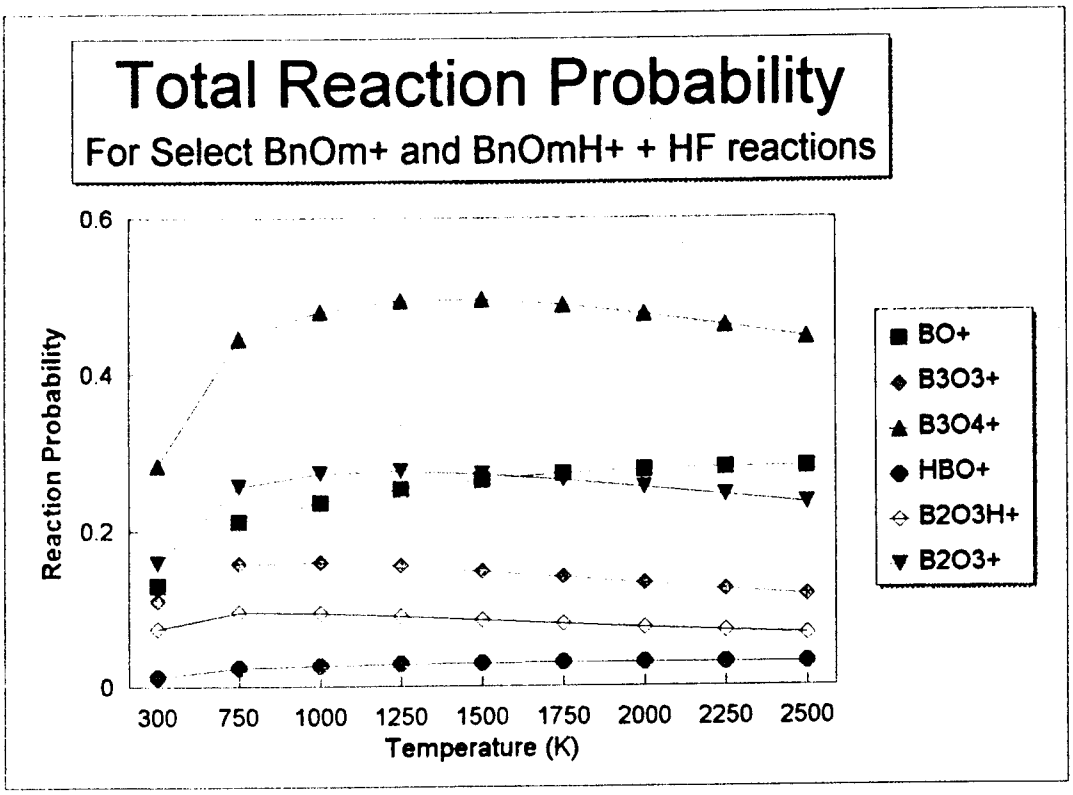
Total Reaction Probability
For Select BnOm+ and BnOmH+ + HF reactions
Reaction Probability
0.6
0.4
0.2
0
300
750
1000
1250
1500
1750
2000
2250
2500
Temperature (K)
BO+
B3O3+
B3O4+
HBO+
B2O3H+
B2O3+

Fig.20

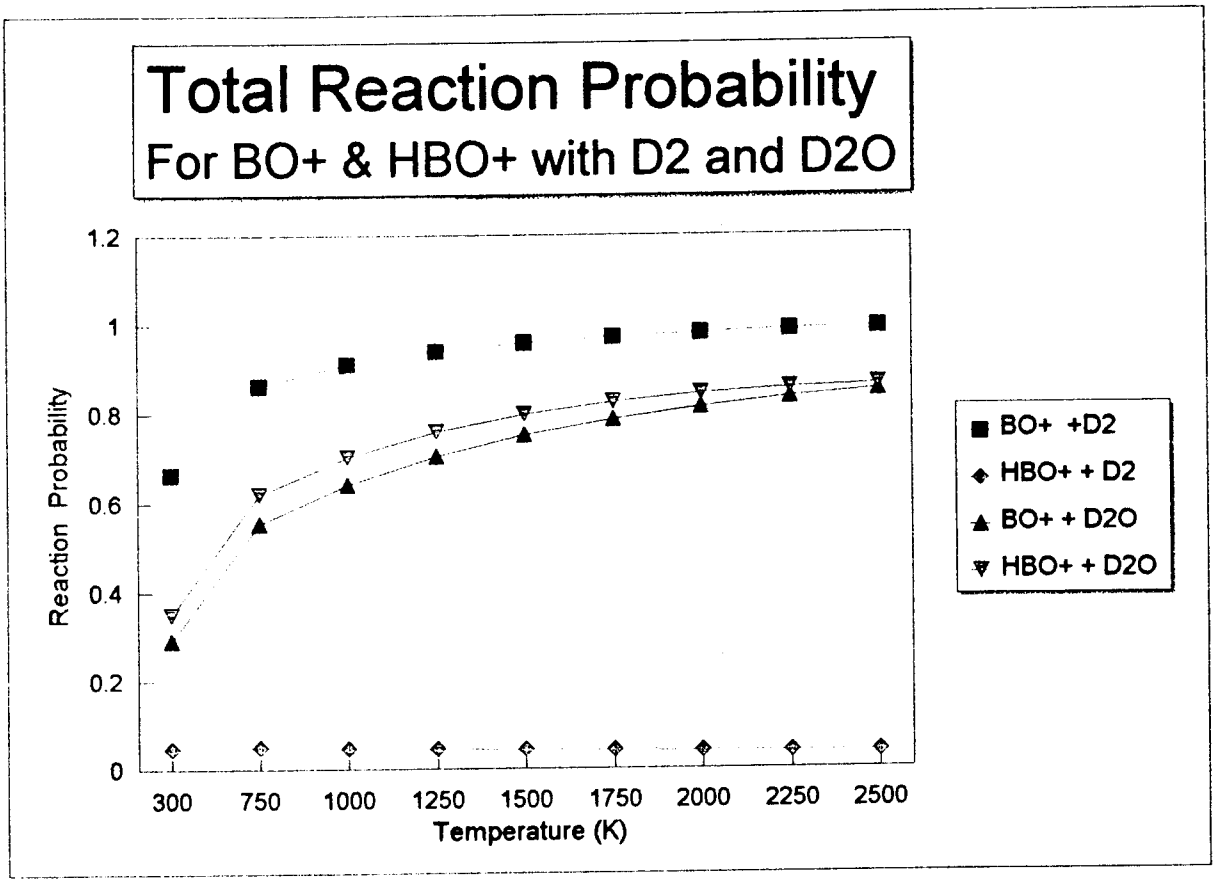
Total Reaction Probability
For BO+ & HBO+ with D2 and D2O
Reaction Probability
1.2
1
0.8
0.6
0.4
0.2
0
300
750
1000
1250
1500
1750
2000
2250
2500
Temperature (K)
BO+ +D2
HBO+ + D2
BO+ + D2O
HBO+ + D2O

Fig.21

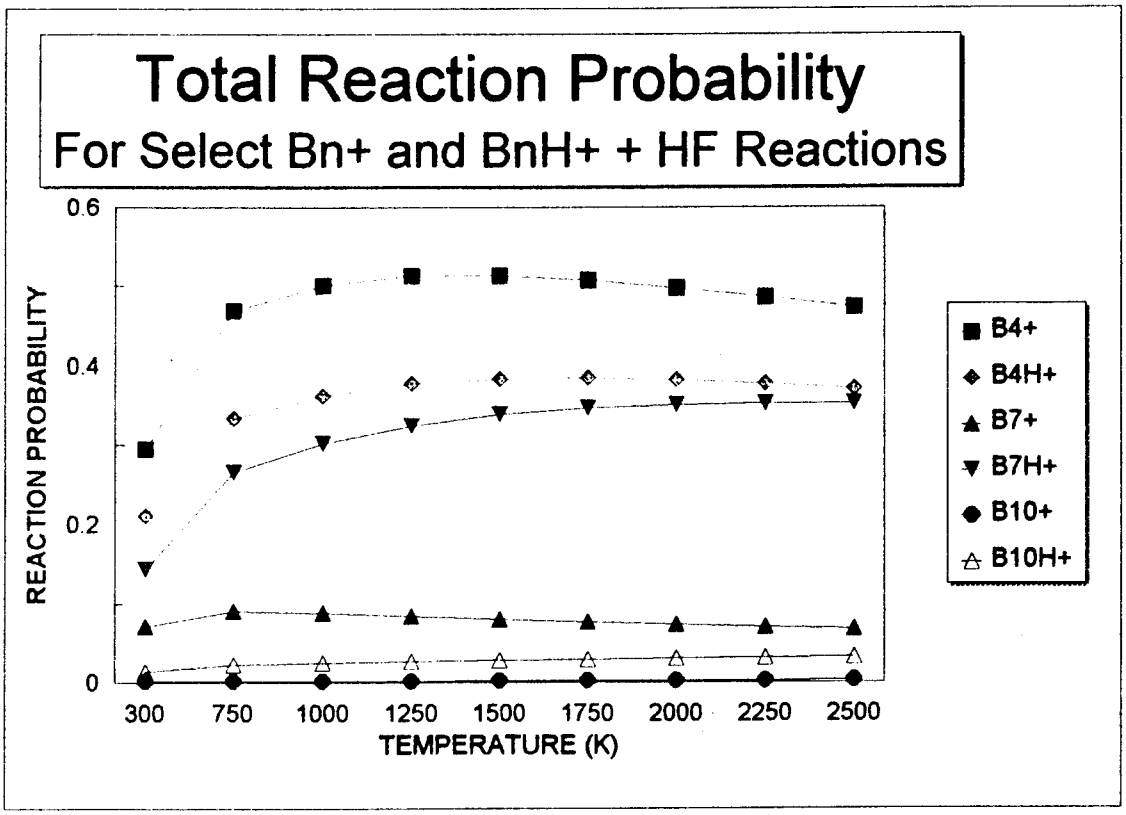
Total Reaction Probability
For Select Bn+ and BnH+ + HF Reactions
REACTION PROBABILITY
0.6
0.4
0.2
0
300
750
1000
1250
1500
1750
2000
2250
2500
TEMPERATURE (K)
B4+
B4H+
B7+
B7H+
B10+
B10H+

Fig.22